



Kent Academic Repository

Cook, Alexander (2016) *Design of a Fluorescent mRNA Biosensor*. Master of Science by Research (MScRes) thesis, University of Kent,.

Downloaded from

<https://kar.kent.ac.uk/57542/> The University of Kent's Academic Repository KAR

The version of record is available from

This document version

UNSPECIFIED

DOI for this version

Licence for this version

UNSPECIFIED

Additional information

Versions of research works

Versions of Record

If this version is the version of record, it is the same as the published version available on the publisher's web site. Cite as the published version.

Author Accepted Manuscripts

If this document is identified as the Author Accepted Manuscript it is the version after peer review but before type setting, copy editing or publisher branding. Cite as Surname, Initial. (Year) 'Title of article'. To be published in *Title of Journal*, Volume and issue numbers [peer-reviewed accepted version]. Available at: DOI or URL (Accessed: date).

Enquiries

If you have questions about this document contact ResearchSupport@kent.ac.uk. Please include the URL of the record in KAR. If you believe that your, or a third party's rights have been compromised through this document please see our [Take Down policy](https://www.kent.ac.uk/guides/kar-the-kent-academic-repository#policies) (available from <https://www.kent.ac.uk/guides/kar-the-kent-academic-repository#policies>).

Design of a Fluorescent mRNA Biosensor

Alexander Cook
MSc. Biochemistry 2016

Supervisor: Dr. Christopher Toseland
School of Biosciences,
University of Kent.

Declaration

No part of this thesis has been submitted in support of an application for any degree or other qualification of the University of Kent, or any other University or Institution of learning.

Acknowledgments

My thanks go to Dr. Chris Toseland for all of the support and advice he has given me throughout my research. He has ignited my interest in biochemistry and encouraged me to stay in the world of academia and research. Without him this research would not have been possible.

I would like to thank Ália dos Santos who has shared her knowledge with me and has encouraged me throughout all of my work.

A big thank you goes to everyone from the Toseland, Goult and Kad lab who took me in when I first arrived and have made my experience here unforgettable. They have shown me what it means to be part of a lab and how important it is to enjoy where you work.

My final thanks of course go to my parents, without them I would not have made it as far as I have. They have provided constant support, food when needed and have provided refuge when work has been tough. I am forever indebted.

Contents

Declaration.....	1
Acknowledgments.....	2
Abbreviations.....	5
Abstract.....	7
Chapter 1: Introduction	8
1.1 Transcription and its importance.....	8
1.2 The process of transcription	8
1.3 <i>In vitro</i> transcription	10
1.4 RNA quantification to study <i>in vitro</i> transcription.....	11
1.5 Methods to study transcription activity in real time	12
1.6 The differences between RNA and DNA.....	13
1.7 Working with fluorescence.....	14
1.8 Current fluorescent biosensors.....	16
1.9 What is SSB?.....	17
1.10 How has it been used previously?.....	19
1.11 Aims	20
2. Methods and Materials.....	21
2.1 Plasmids used	21
2.2 Oligonucleotides used.	22
2.3 Expression of SSB.....	23
2.4 Purification of SSB.....	Error! Bookmark not defined.
2.4.1 Polymin P and Ammonium sulfate precipitation.....	29
2.4.2 Heparin Column with a Gel Filtration column.	30
2.4.3 Ammonium sulphate precipitation with a Q sepharose column.....	31
2.4.4 His-tagged SSB	32
2.5 Eletrophoretic Mobility Shift Assay (EMSA)	23
2.6 Tryptophan fluorescence titration.....	23
2.7 Nanotemper Tryptophan florescence titration	24
2.8 Titration of SSB into fluorescein nucleotides.....	24
2.9 Labelling SSB monomers with MDCC.....	24
2.10 Signal to noise fluorescence measurements of MDCC-SSB	25
2.11 Titrations of Oligonucleotides to MDCC-SSB	25
2.12 PcrA helicase assay with dsDNA	26
2.13 Competition assay.....	26
2.14 Post transcription analysis using SSB	26

2.15	Real time transcription analysis.....	27
2.16	Circular Dichroism (CD) analysis.	27
2.17	Dynamic light scattering analysis (DLS).....	28
2.18	Photostability of MDCC.....	28
3.	Results.....	29
3.1	Proving SSB does bind to mRNA.....	33
3.2	The design of the MDCC-SSB biosensor.	40
3.3	Testing the biosensor	40
3.3	Characterisation of the MDCC-SSB biosensor	45
3.4	Application of MDCC-SSB biosensor to measure <i>in vitro</i> transcripts.....	48
3.5	Evaluating the loss of fluorescence	52
4.	Discussion.....	57
4.1	SSB can bind RNA substrates	57
4.2	Generating the biosensor	60
4.3	Application of the biosensor	62
5.	Further Work.....	64
6.	Appendix	66
7.	References	67

Abbreviations

mRNA	Messenger Ribonucleic Acid
RT-qPCR	Reverse Transcription – quantitative PCR
<i>E. coli</i>	<i>Escherichia coli</i>
SSB	Single Stranded Binding protein
<i>et al</i>	Et alia
ssDNA	Single stranded DeoxyRiboNucleic Acid
ssRNA	Single stranded Ribonucleic Acid
dsDNA	double stranded DeoxyRiboNucleic Acid
rRNA	Ribosomal RiboNucleic Acid
miRNA	micro RiboNucleic Acid
tRNA	transfer RiboNucleic Acid
<i>S. typhimurium</i>	<i>Salmonella typhimurium</i>
FRET	Förster resonance energy transfer
UTR	UnTranslated Region
IUPAC	International Union of Pure and Applied Chemistry
ATP	Adenosine TriPhosphate
PcrA	Plasmid Copy Reduced A
OB-fold	Oligonucleotide/Oligosaccharide-Binding fold
M	Molarity (moles per litre)
mM	Milli-Molar
µM	micro-Molar
nM	nano-Molar
pM	pic0-Molar
G	Glycine
C	Cysteine

MDCC	7-Diethylamino-3-(((2-Maleimidyl)ethyl)amino)carbonyl)coumarin
LB	Lysogeny Broth
IPTG	Isopropyl β -D-1-thiogalactopyranoside
PMSF	Phenylmethanesulfonyl fluoride
Polymin P	Polyethyleneimine
EDTA	Ethylenediaminetetraacetic acid
SDS-PAGE	Sodium Dodecyl Sulfate - PolyAcrylamide Gel Electrophoresis
μ l	micro-litre
mg	milligram
DTT	Dithiothreitol
nm	nanometre
His	Histidine
Da	Dalton
kDa	kiloDalton
OD ₆₀₀	Optical Density at 600nm
PBS	Phosphate Buffered Saline
mgmL ⁻¹	milligram per millilitre
UV	Ultraviolet light
s	second
min	minute
MW	Molecular Weight
l	pathlength
c	concentration
CD	Circular Dichroism
DLS	Dynamic Light Scattering

Abstract

Currently, to measure the amount of mRNA produced during transcription, a post transcription assay is required, such as gel electrophoresis or reverse transcription- quantitative polymerase chain reaction (RT-qPCR) which all require RNA purification steps. Both methods are subject to high error and in addition, RT-qPCR is a long process which can take hours to run. This study describes a method in which post transcriptional mRNA can be qualitatively measured between reaction conditions or quantitatively measured after calibration. The post transcription assay utilises a fluorescent *Escherichia coli* single stranded binding protein (SSB). In this study, SSB showed similar binding properties to mRNA, to that of its native substrate, ssDNA. A mutant of SSB -SSB G26C- used in previous studies, was fluorescently labelled with 7-Diethylamino-3-(((2-Maleimidyl)ethyl)amino)carbonyl)coumarin (MDCC). A fluorescence increase occurs when the SSB is bound to both ssDNA and ssRNA, and this increase is dependent on substrate concentration. This study shows the MDCC-SSB can be used as a comparative measurement of mRNA concentrations following *in vitro* transcription. After finding this method unsuitable for real time studies, we investigated potential causes for this behaviour and comment on improvements to the biosensor.

Chapter 1: Introduction

1.1 Transcription and its importance

Transcription is the decoding of the DNA into RNA and is at the cornerstone of a cell's survival. For transcription to occur large protein complexes are required and transcription factors are needed to direct the transcription. The main component of transcription is the RNA polymerase and in eukaryotes, there are three - RNA polymerase I, II and III. Each of these polymerases are responsible for the production of different types of RNAs. rRNA is transcribed by RNA polymerase I^{1,2}, RNA polymerase II is responsible for transcribing mRNA, miRNA and other certain types of messenger RNA^{2,3} whilst finally RNA polymerase III transcribes tRNA molecules^{2,4}. All three RNA polymerases have different distributions within the nucleus; RNAPI is found in the nucleoli⁵, whilst the remaining two are found in discrete sites around the nucleoplasm^{6,7}. If errors occur within this transcription phase, cells can begin to form tumours⁸ and long non-coding RNAs can lead to certain cancers⁹. For this reason, this makes transcription an important process to study and it is vital to understand the role of every component. One example would be myosin, a known component of transcription machinery, whose role is yet to be understood¹⁰ and so new methods to characterise this element, are necessary. The aim of this study is to produce a reagentless mRNA biosensor that can be used to study transcription *in vitro*, allowing for the rapid and accurate report on polymerase activity, in controlled conditions.

1.2 The process of transcription

Transcription is a process that can be broken into three major stages; initiation, elongation and finally termination. Initiation occurs when an RNA polymerase is recruited to a set promoter sequence within the DNA. This recruitment occurs through interactions with specific transcription factors. In the case of the eukaryotic RNA polymerase II, transcription factors such as TFIIA, TFIIB, TFIID, TFIIE, TFIIIF and TFIIH lead to the formation of the preinitiation complex¹¹ (figure 1.1). This complex of RNA polymerase

and transcription factors is able to trap the promoter DNA open¹². The RNA polymerase is then released from the promoter sequence through various mechanisms, such as interactions of the capping enzyme¹³ and transcription factor interactions including ATP hydrolysis¹⁴. During this period of time the RNAP undergoes repetitive abortive initiation, producing small RNA molecules. Once this newly synthesised RNA reaches a length of approximately 9-11 nucleotides long it enters the elongation stage of transcription¹⁵.

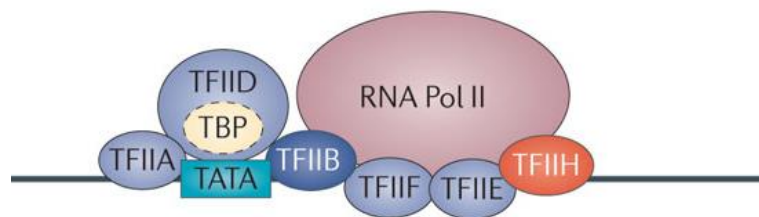


Figure 1.1 **Diagram showing initiation complex of RNA polymerase II.** RNA polymerase II is recruited to the DNA by the array of transcription factors which first bind to the DNA promoter sequence. Adapted from Bywater *et al.*, (2013).¹⁶

The elongation stage is made up of a simpler complex in which, as RNAPII travels along the DNA template, the DNA becomes unwound within the transcript bubble of RNAPII. Nucleoside triphosphates (NTPs) are then polymerised by the RNAPII, forming the RNA transcript from the unwound DNA template (figure 1.2). RNAPII also requires the elongation factors TFIIF and TFIIIS which aid in transcript cleavage, as well as relieving arrest of the RNAPII¹⁷. Once elongation is completed and the RNAPII reaches a termination sequence, the process is terminated and the RNA transcript is then released. This RNAPII transcription process produces a complete mRNA transcript that contains at either end, two untranslated regions (UTR), which stabilise the mRNA but are not translated.

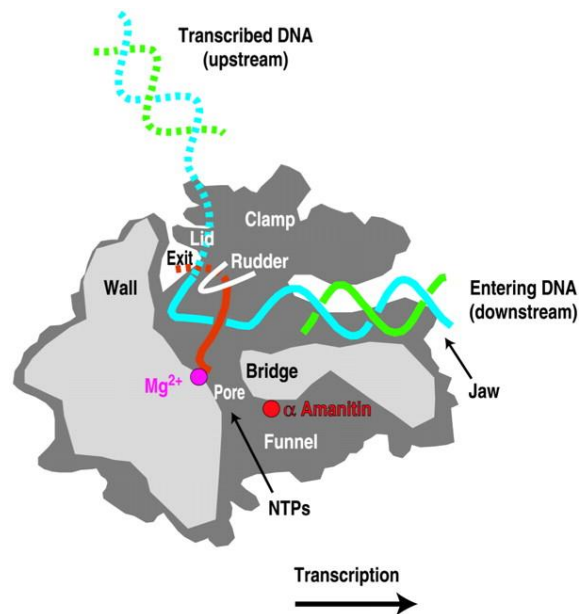


Figure 1.2. **Diagram of RNAPII during elongation.** Downstream DNA enters from the right of the diagram as NTPs enter from below. Polymerisation of the NTPs occur in the centre of the protein and the mRNA transcript in red exits towards the back of the diagram. Diagram adapted from Bushnell, Cramer and Kornberg (2001)¹⁸.

1.3 *In vitro* transcription

To understand which components are required for transcription it is possible to remove them one by one. However, in cells due to their multi part nature, this strategy could lead to complete cell failure through various mechanisms rather than being directly caused by the loss of transcription machinery. Therefore, *in vitro* transcription assays allow for these removal and addition assays without the complexity of the whole nucleus. Transcription kits were first used to produce RNAs back in the late 1980's¹⁹, utilising simple prokaryotic systems. These assays allow laboratories to produce in house RNA to be used for structural analysis as well as RNAi²⁰ and the reprogramming of cells to pluripotency²¹. It also focuses on the basic requirements for transcription and removes the excess nuclear environment, allowing for the study of transcription and the activity of the RNA polymerase only. Three basic prokaryotic polymerases have been well characterised for *in vitro* transcription. The *E. Coli* phages T3²² and T7²³, and *S. typhimurium* SP6 polymerases²⁴. Within this study the T7

polymerase has been employed to act as our model of transcription ensuring the assay works before applying it to an *in vitro* eukaryotic transcription assay. Eukaryotic transcription assays are slightly different due to the fact they rely on nuclear extracts that are able to undergo RNA polymerase II transcription through different selective measures²⁵, but this system still contains unnecessary impurities and uncharacterised components.

1.4 RNA quantification to study *in vitro* transcription

The classical methods to study *in vitro* transcription, detect the presence or quantify the mRNA transcripts produced. In high yielding transcription assays such as the T7 polymerase, the presence of mRNA can be shown by undergoing RNA purification and then separating the transcripts using agarose gel electrophoresis, followed by staining with a common nucleotide stain such as SYBR®Gold (Invitrogen, Rochford UK). If the analysis requires quantification of RNA a simple nanodrop is able to measure nucleic acid concentration and purity through the absorptions between wavelengths 230nm-340nm²⁶. However, for both these methods samples need to undergo RNA purification to remove both proteins and DNA from the solution, this always leads to loss of total RNA yield. The methods described require high yields of mRNA product and therefore are not suitable for eukaryotic transcription assays. The use of radioactively tagged nucleotides and quantitative PCR (qPCR) are the two most common methods to measure eukaryotic *in vitro* transcription. Isotopically labelled ³²P (phosphorous) is a common label incorporated into nucleotides that are assimilated into mRNA during *in vitro* transcription and allows for the quantification of transcript produced²⁷, this method though can be costly and requires appropriate safety gear as well as a scintillation counter. There are slight variations of qPCR; however, one method, reverse transcription quantitative PCR (RT-qPCR) is able to utilise specific fluorescently tagged primers that bind to the cDNA, produced from the reverse transcription of the mRNA transcribed, during PCR²⁸. Once again, this method has drawbacks due to the multi-step process for purifying mRNA, the design of primers and the reverse transcription step, all of which takes time and can cause the loss of transcribed mRNA. More modern approaches such as QuantiGene is a

multi-step process in which the mRNA samples do not need to be purified but are trapped to framework and then probed and stained²⁹. Quant-iT™ RiboGreen® RNA reagent, another modern approach to mRNA quantification, is a dye that relies on the fluorescence increase of around 1000-fold when bound to RNA and results in an RNA concentration dependent fluorescence increase³⁰. All methods stated, except for that of the QuantiGene, require mRNA purification and none of them are able to study transcription in real time.

1.5 Methods to study transcription activity in real time

To fully understand the transcription process it is vital to study it in real time. If transcription could be followed in real time, it would be possible to design experiments in which, with the addition of inhibitors, the removal of transcription factors or the varying of other necessary components, allowing for the immediate effects on transcription to be analysed. As previously discussed, RNA quantification takes brief snap shots of the transcription process and so, depending on the timing of these snapshots, different phases of transcription could be misconstrued. Currently there are few accessible methods to study transcription in real time *in vitro* and so it is necessary to look at *in vivo* methods to present an *in vitro* method. RNA transcription can be visualised *in vivo* through light up and FRET aptamers^{31,32}. These consist of designed nucleic acids able to bind tightly to RNA, causing a visible fluorescence increase. This method allows us to trace RNA progression through cells and can provides a total amount of the specified RNA being transcribed. Nuclear run-on analysis³³ of transcription provides direct measurement of one gene and utilises RNA polymerase II to incorporate radioactive nucleotides into the gene. The amount of incorporation reflects a direct link to transcriptional activity of RNA polymerase II on that specific gene similar to that of the *in vitro* method. This method however requires complete and isolated nuclei and of course uses potentially harmful and expensive radioactive substances. Whilst all of these methods are *in vivo* very little has been designed to measure *in vitro* where conditions and transcription components can be controlled. 2'-O-methylribonucleotide molecular beacons have been used *in vitro* to study transcription of different RNA polymerases³⁴. This method requires specifically designed beacons to be synthesised to match the known transcript. As

well as specific synthesis, the beacons require unnatural amino acids which are expensive and hard to synthesise. Binary probes as a FRET pair is method that has been built on molecular beacons to measure transcription activity *in vitro* and in real, these are created to specifically bind to either the 5' or 3' UTR and use Cy3 and Cy5 as FRET fluorophores³⁵. This real time method does show transcriptional activity through mRNA production and whilst relies less on gene specificity, its' FRET signal depends on the UTR sequence used and its environment due to varying degrees of hybridisation. None of these methods are reagentless and they have large variations of results depending on the mRNA transcript.

1.6 The differences between RNA and DNA

To produce a biosensor and a protocol that is able to distinguish between the different components present in the transcription solution, it is important to understand the differences between the mRNA transcript and the DNA template. As previously mentioned it is already possible to quantify RNA and DNA independently; however, some methods are unable to distinguish either between the two or between the different varieties of RNA. Loss of the second alcohol group on the 2' of the ribose sugar and replacement it with a simple hydrogen results in simple ribose sugar which is the difference between DNA and RNA and it is this difference that leads to their significantly separate roles. It is because of these differences that it is vital to segregate the two when undergoing *in vitro* quantification of RNA. Whilst UV quantification is rapid and easy it is unable to distinguish between RNA and DNA and is only able to measure total nucleotide concentration. To ensure reliable concentration readings the RNA needs to be purified. As both single stranded and double stranded nucleic acids are present in transcription, it is a must to create a biosensor that can be specific only to the single stranded nucleic acids- mRNA. Most common nucleic dyes to quantify RNA struggle to differentiate between DNA and RNA. Secondly, if possible the sensor needs to identify specifically mRNA and not any other forms such as tRNA. This is where the RiboGreen® dye has its downfall as it is able to bind to all forms of RNA³⁰. We wish to distinguish between all of these because the mRNA

concentration reflects solely on the polymerase activity and should be the only measurable variable in the system. The *in vitro* eukaryotic transcription systems could potentially have various RNA species that could cause false positives, if the RiboGreen® was used.

1.7 Working with fluorescence.

The use of fluorescence as a technique has increased rapidly in recent years due to its particular properties and has been employed in this study. Fluorescence is used from imaging³⁶, to measuring kinetics of binding partners³⁷ and to acting as a sensor for certain substrates³⁸. Fluorescence is so widely applied for various reasons: it is a much safer choice over radioactively labelled options that require appropriate containment and disposal, and it has a high sensitivity within biochemical assays that allow measurements of protein interactions from micromolar to low picomolar^{39,40}. The signals are rapid, allowing sensitive single molecule studies. Single molecule studies use fluorescence to visualise single interactions and association kinetics of proteins binding to their specific substrates, such as the recruitment of fluorescently tagged transcription factors to DNA⁴¹. When using a fluorescent marker for any of these techniques, various qualities have to be assessed. Fluorescence is emitted from a molecule after it has been excited by absorbing a photon, as it releases the photon and returns to its ground state it emits fluorescence at a longer, lower energy wavelength than absorbed as shown in figure 1.3.

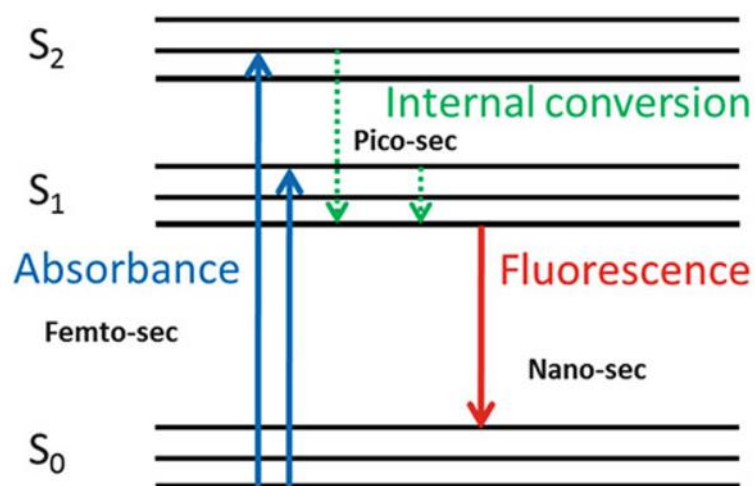


Figure 1.3. **Jablonski energy diagram of fluorescence.** Absorbance of a photon takes a femto-second, energy is absorbed by the molecule and the photon is released at a lower energy wavelength taking approximately a nano-second. Taken from Fili & Toseland. (2014)⁴².

When first evaluating the fluorescence of a molecule it is important to define its excitation and emission wavelengths and ensure the Stokes shift is appropriate for its application. Stokes shift is the difference between the excitation and emission maximum wavelengths, if these are too similar it is not possible to detect the emission without large background readings from the exciting light source. This can mean that different instrumentation such as bulbs and filters may need to be altered. Secondly, when deciding on fluorescent molecules the life-time of the emission and the stability of the fluorophore need to be taken into consideration. Bleaching of fluorophores can occur over time and so the fluorescent signal can reduce, giving false or incorrect measurements which is of particular importance for slow processes. Finally, brightness needs to be considered, if the dye is used for imaging, then a much brighter dye is required compared to that used in stopped flow where brightness of a fluorophore can lower. In this study the thiol reactive coumarin dye 7-Diethylamino-3-(((2-Maleimidyl)ethyl)amino)carbonyl)coumarin (MDCC) was deemed a suitable fluorophore as it is very stable. Whilst it is not ideal for microscopy due to its poor photophysical properties, it is suitable for more sensitive biochemical studies.

1.8 Current fluorescent biosensors

Biosensors have been defined by IUPAC as “a specific type of chemical sensor comprising a biological or biologically derived recognition element,”⁴³ and, like with any type of sensor, is comprised of two elements. The first being the recognition element, this needs to be able to specifically recognise the substrate and have some interaction with it. The remaining component is the transducer, which leads to a measurable signal, in the case of this study, the transducer is the fluorescent molecule. In the case of biosensors, often the biological component is the recognition element which can be derived from proteins⁴⁴, aptamers⁴⁵ and anti-bodies⁴⁶. In this study a protein based biosensor has been created and so will be the focus from now on. Protein based biosensors utilise the highly evolved specificity that has already been well characterised for that protein. For example in the production of an inorganic phosphate biosensor Brune *et al*⁴⁷ manipulated the specificity of the phosphate binding protein and attached a fluorescent dye. As a result, once the protein was bound to an inorganic phosphate (P_i), a 13 fold increase in fluorescence intensity was observed and this was later used to measure the activity of actomyosin subfragment 1 ATPase⁴⁸. Another example of where proteins have been selected for their specificity was in the production of a real time biosensor for helicase activity. Dillingham *et al*⁴⁹ used the single stranded binding protein from *E. coli* tagged with a fluorescent dye, that bound to single stranded DNA as the helicase PcrA unwound dsDNA. This allowed helicase activity and the speed of which it unwound dsDNA to be measured in a reagentless fashion and in real time. This was then taken a step further with helicase activity being visualised in single molecule studies⁵⁰. By requiring only the protein to be in the sample mixture and no other extra reagents necessary it is possible to keep the conditions near native and with SSB being naturally found in the cell it does not intervene with the helicase process. From these previous studies we have wanted to apply the same tactics used and utilise SSB as the biosensor to bind and measure mRNA.

1.9 What is SSB?

To ensure the SSB was an appropriate protein to use as an mRNA fluorescence biosensor it is important to understand its stability and interactions in different environments. *E. coli* SSB is a well characterised protein that is homo-tetrameric and contains 4 OB-fold domains⁵¹. Oligonucleotide binding folds (OB-folds) can be β -barrels consisting of 5 highly coiled antiparallel β sheets and vary in length across OB-fold containing proteins, as well as this they also have a very low degree of similarity in their sequence between themselves⁵². There is one of these OB-fold domains, responsible for the ssDNA binding of each monomer. These monomers are each 18.9kDa large. One main use for SSB in the cell is that its C-terminal binding domains have shown to be the biologically important domains responsible for DNA replication and repair⁵³. The formation and binding properties of SSB vary depending on the surrounding conditions. It has two main binding modes, known as (SSB)₆₅ and (SSB)₃₅, which have been well characterised by Lohman *et al*⁵⁴. In high salt concentrations above 200mM NaCl SSB binds to ssDNA in the form of (SSB)₆₅, this means that all four OB-folds are bound to ssDNA. This case is also true when the nucleotide length is approximately 65 nucleotides long, causing the ssDNA to wrap completely around the protein. (SSB)₃₅ however is a different bonding mode where the ssDNA wraps only around half of the protein and interacts with only two of the four OB-folds. This binding mode occurs in low salt concentrations less than 200mM NaCl and when the nucleotide length is around 35⁵⁵ as shown in figure 1.4. In the case of (SSB)₃₅ it is possible for two ssDNA molecules that are 35 nucleotides long are able to bind to one SSB tetramer⁵⁶. It has recently been shown that both these binding modes can lead to normal cell growth and therefore it is likely that both exist in the cell⁵⁷.

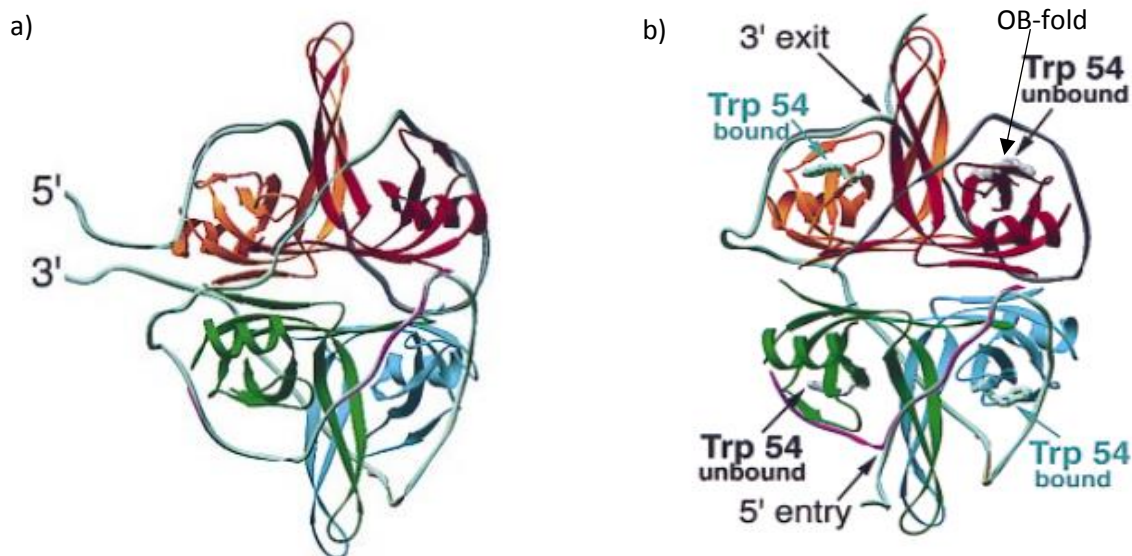


Figure 1.4. **SSB in its bound states.** a) (SSB)₆₅ bound to ssDNA with full wrapping and all four OB-folds interacting. b) (SSB)₃₅ bound to ssDNA with half wrapping and only two OB-folds interacting showing the 5' below the protein and 3' above compared to (SSB)₆₅ where both ends are adjacent. Taken from Raghunathan *et al.*, (2000)⁵⁸.

(SSB)₃₅ is able to undergo what has been classified as unlimited cooperativity with ssDNA, which is the formation of proteins lined along the piece of ssDNA. (SSB)₆₅ undergoes limited cooperativity because all four OB-fold interactions lead to an irregular pattern of dimerised proteins (figure 1.5)⁵⁹. All of these binding modes need to be taken into account when using SSB as a biosensor, as depending the placement of the fluorophore and its local environment can all have an effect on the fluorescence change that could occur. SSB has also shown to have incredibly tight binding to ssDNA⁶⁰ and, whilst not as tightly as with ssDNA, SSB is also able to bind to RNA of different lengths and types, with varying strengths⁶¹. Due to these different binding modes and the varying salt concentrations in transcription assays, it is important to consider both binding modes when preparing the biosensor.

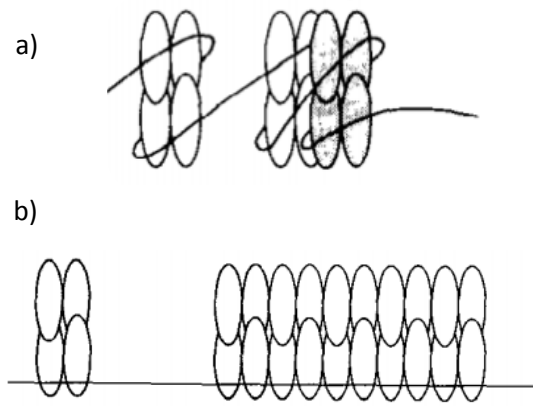


Figure 1.5. **Two types of cooperativity of SSB bound to ssDNA.** a) Limited cooperativity of (SSB)₆₅ shown with only formation of dimer tetramers. b) Unlimited cooperativity of (SSB)₃₅ able to bind repetitively adjacent to each other. Adapted from Lohman, T. M. & Ferrari M. E. (1994).⁵⁴

1.10 How has it been used previously?

As previously mentioned, SSB has already been used as a biosensor to report on the unwinding of helicases. By carrying on the previous work done by Dillingham *et al.*⁴⁹, this study will use the same point mutated SSB in which a glycine residue is replaced by a cysteine residue at the 26th position. This mutation does not affect the binding of SSB or the formation of its tetrameric shape⁴⁹. When SSB is referred to in this study, it is assumed the reference is to the G26C mutant. This mutation allows for the thiol reactive fluorophore N-[2-(iodoacetamido)ethyl]-7-diethylaminocoumarin-3-carboxamide (IDCC) to be attached. By having the fluorescent dye at this position, a fluorescence increase was observed by Dillingham *et al.*⁴⁹, due changes in the local environment, when SSB binds to ssDNA. Whilst IDCC is not currently available from manufacturers, in this study the commercially available fluorophore, MDCC was used to ensure the mRNA biosensor is easy to produce. Both dyes are comprised of the same functional groups, however, MDCC comes in two isomers compared to IDCC which is a completely fixed structure. The fluorescence properties of both MDCC isomers have not been characterised separately and, therefore may vary between each other, leading to a variation of fluorescence emission within samples.

1.11 Aims

This study aims to build upon previous ideas and methods to show that SSB, whilst already proven to be a strong reagentless biosensor for ssDNA, can also be used to measure mRNA concentration. This will allow for the real time analysis of RNA polymerases as shown in figure 1.6 and the production of a biosensor that can be produced relatively cheaply without any specialist equipment.

This project can be broken down into the following definitive aims:

- 1) Characterise SSB ssRNA binding.
- 2) Utilise MDCC-SSB as a post transcription biosensor to qualitatively analyse the concentration of mRNA so as to act as a quick and easy mRNA measurement method.
- 3) Show that calibration can be undertaken with MDCC-SSB to allow for the quantification of mRNA in transcription samples.
- 4) To use MDCC-SSB in a real time transcription assay allowing the RNA polymerase activity to be measured.

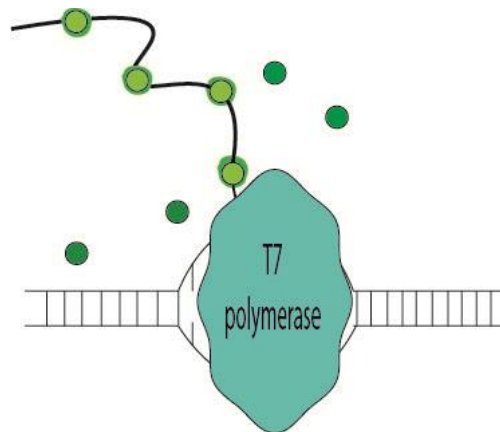


Figure 1.6. A schematic to show MDCC-SSB in green increasing in fluorescence when bound to mRNA as it is transcribed by the T7 polymerase.

2. Methods and Materials

2.1 Reagents

Unless stated otherwise all reagents were purchased from Sigma Aldrich (Dorset, UK).

2.2 Plasmids used

Plasmid	Type	Marker	Supplier
G26C SSB	pET28 (No tag)	Ampicillin	Provided by Dillingham <i>et al</i> ⁴⁹
G26C SSB His-tagged	pET151 (His tag)	Ampicillin	Life technologies (California, USA)

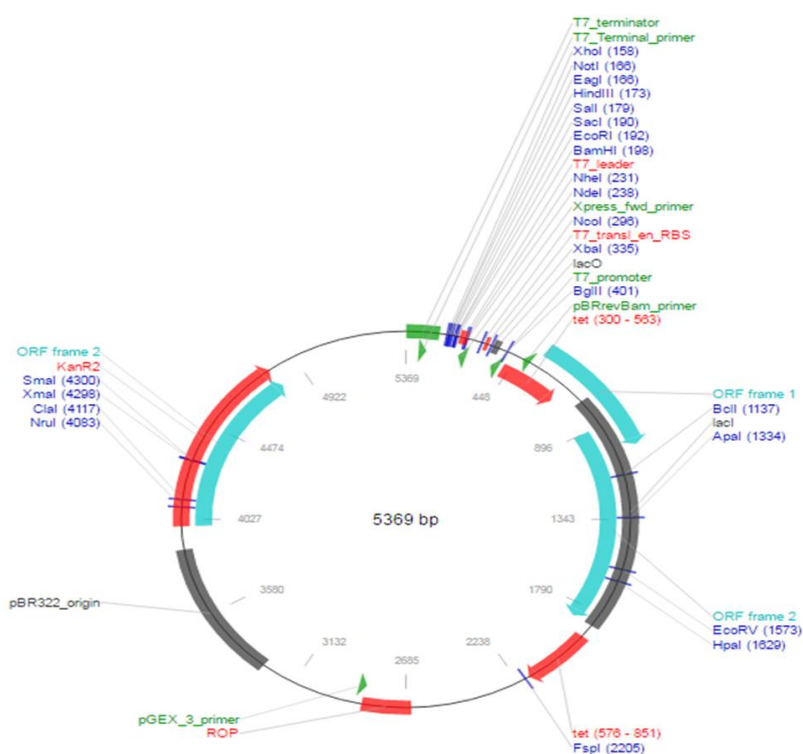


Figure 2.1. **Plasmid map of pET28.** The plasmid was provided by Dillingham *et al.*,⁴⁹ with the gene inserted between the T7 promoter and terminator.

2.4 Expression of SSB

E.coli BL21 competent cells were transformed with the designated vector using the heat-shock method⁶² and were grown overnight in Lysogeny Broth (LB) with 100 µg. mL⁻¹ ampicillin at 37°C and at 280 rpm. A 10mL aliquot of cells were then placed into 1 litre of fresh LB with 100 µg. mL⁻¹ ampicillin and allowed to grow in the same conditions until a cell OD₆₀₀ of 0.6 was reached. Cells were then induced with 1mM IPTG. After induction cells were grown over night at 18°C. Cells were centrifuged at 4000rpm for 20 minutes at 4°C and resuspended in resuspension buffer (50mM Tris.HCl pH 7.5, 40mM imidazole, 200mM NaCl, 1mM DTT and 20% sucrose) and 0.1mM PMSF and stored at -20°C.

2.5 Electrophoretic Mobility Shift Assay (EMSA)

50nM SSB was incubated with 250nM ssDNA₇₀ or ssRNA₇₀ for 20 minutes at room temperature in 50mM Tris.HCl pH 7.5, 100mM NaCl, 3mM MgCl₂. Samples were loaded onto an acrylamide gel (12% acrylamide, Tris. Boric acid pH 7.5) (TB) and ran in TB buffer. SYBR®Gold (Invitrogen, Rochford, UK) stained the nucleic acids following the manufacturer's instructions.

2.6 Tryptophan fluorescence titration

10nM of ssDNA₇₀ or ssRNA₇₀ were titrated into 200nM SSB at 25°C in 50mM Tris.HCl pH 7.5, 100mM NaCl or 200mM NaCl as defined and 2mM MgCl₂. Tryptophan fluorescence was measured using a Cary Eclipse Fluorescence Spectrophotometer (Agilent, Edinburgh, UK) at excitation 285nm and emission at 325nm. To calculate fluorescence quenched (%) used equation 1.

Equation 1)
$$\text{Fluorescence quenched (\%)} = \frac{F_i \times DF_i}{F_0} \times 100$$

Where F_0 is initial fluorescence intensity, F_i is the intensity after titration and DF_i is the dilution factor from the titration. The titration curves were fit with two linear regression lines using Grafit (Erathicus, Horley, UK) and their interception calculated.

2.7 Nanotemper Tryptophan fluorescence titration

200nM SSB was incubated with 16 capillaries containing varying concentrations of substrate as defined from 1 μ M to 0.1nM at room temperature in 1X Phosphate buffer saline (PBS). Tryptophan quenching was measured using the Monolith NT. Label free fluorometer (NanoTemper technologies, Munich, Germany) at room temperature whilst under supervision from a representative of the company. The result was presented by the representative after using software provided.

2.8 Titration of SSB into fluorescein nucleotides.

100 μ l of 1 μ M fluorescein nucleotides of varying length and type (table 2.2) were aliquoted into a 96 well plate and serial diluted with SSB (1-0 μ M) in 50mM Tris.HCl pH 7.5, 100mM NaCl, 3mM MgCl₂. The fluorescein was excited at 489nm and fluorescence was measured using a ClarioStar microplate reader (BMG LabTech, Ayelsbury, UK) from 520nm to 600nm. The fluorescence intensity was corrected for dilutions and then normalized, with the highest intensity being 1.

2.9 Labelling SSB monomers with MDCC

The labelling method has been adapted from Dillingham *et al*⁴⁹. 3mg of SSB was incubated with 1M DTT for 20 minutes at room temperature. A PD10 column (GE Healthcare, Little Chalfont, UK) was equilibrated in 20mL of 20mM Tris.HCl pH 7.5, 1mM EDTA, 500mM NaCl and 20% glycerol. After DTT incubation the solution was loaded onto the column and the column was eluted with the same buffer. The A₂₈₀ was measured for each fraction and samples containing SSB were pooled together. 2 fold molar excess of MDCC was added and incubated at defined conditions with end over end mixing and in protection from light. A new PD10 column was equilibrated in 20mL of 20mM Tris.HCl pH 7.5, 1mM EDTA, 500mM NaCl and 20% glycerol and the MDCC-SSB was loaded onto the column, and washed and eluted using the previous buffer removing any excess MDCC. The concentration of SSB was taken using A₂₈₀ absorption with extinction coefficient of $\epsilon = 28,500 \text{ cm}^{-1} \text{ M}^{-1}$ per monomer and MDCC

concentration was taken using absorption at 435nm and the extinction coefficient is assumed to remain the same at $50,000 \text{ cm}^{-1} \text{ M}^{-1}$. To calculate labelling efficiency equation 2 was used.

$$\text{Equation 2) } \textit{Labelling efficiency} = \frac{A_x}{\epsilon} \times \frac{\textit{MW of protein}}{\textit{mg protein/mL}} = \frac{\textit{moles of dye}}{\textit{moles of protein}}$$

Where A_x is the absorbance value of the dye at the absorption maximum wavelength. ϵ is the molar extinction coefficient of the dye at absorption maximum wavelength. SDS-PAGE analysis then showed the protein at the expected molecular weight of approximately 19,270 Da.

2.10 Signal to noise fluorescence measurements of MDCC-SSB

2 μM MDCC-SSB subunits were serially diluted in 100 μl of 50mM Tris.HCl pH 7.5, 3mM MgCl_2 and 100mM or 200mM NaCl as defined in a 96 well plate. For strength of signal to noise ratio a concentration of MDCC-SSB ranged from 0-0.25 μM and both excitation and emission were measured from 400nm-440nm and 455nm-550nm respectively, using a ClarioStar microplate reader (BMG, LabTech, Ayelsbury, UK).

2.11 Titrations of Oligonucleotides to MDCC-SSB

1 μM of ssDNA₇₀/ssRNA₇₀ was serial diluted across 10 wells of 100 μl of 50nM MDCC-SSB in 50mM Tris.HCl pH 7.5, 3mM MgCl_2 and 100mM or 200mM NaCl as defined. The fluorescence intensity was then taken at 471nm. Fluorescence change is presented as a ratio using equation 4.

$$\text{Equation 4) } \textit{Fluorescence change} = \frac{F_i \times DF_i}{F_0}$$

Where F_0 is initial fluorescence intensity at 471nm and F_i is the intensity at 471nm after titration. DF_i is the dilution factor for that titration.

2.12 PcrA helicase assay with dsDNA

20nM RepD was added to 5nM dsDNA in 50mM Tris.HCl pH 7.5, 100mM KCl and 10mM MgCl₂ and incubated at 30°C for 15 minutes. 100nM of the helicase PcrA and 50nM of MDCC-SSB was then added and incubated at 30°C for 2 minutes. 1mM of ATP was then added to the mixture and 100µl of solution was placed in a well of a 96 well plate and incubated in the ClarioStar microplate reader at 30°C. Fluorescence emission taken at 470nm was measured every 30 seconds for 15 minutes.

2.13 Competition assay

50nM fluorescein ssDNA₄₀ (fssDNA₄₀), 50nM fssDNA₄₀ with 75nM SSB and 75nM SSB with 1µM ssRNA₇₀ were set up respectively in individual wells in a 96 well plate. The fluorescence emission of all three were measured using the Clariostar microplate reader from 515nm to 600nm at 25°C. 50nM of fluorescein ssDNA₄₀ was then added to the solution containing 1µM ssRNA₇₀ and the fluorescent intensities were re-measured using the same conditions. Fluorescence emission was then normalised to 1; 1 being the highest intensity of the free fluorescein ssDNA₄₀.

2.14 Post transcription analysis using SSB

Post transcription was undertaken using the HiScribe™ T7 High Yield RNA Synthesis Kit (New England Biolabs, Hitchin, UK) and the template RecD2 gene which produces a transcript 2225nt long. The transcription was ran for various lengths of time to produce different amounts of transcript. RNA was then purified using RNeasy® kit (Qiagen, Manchester, UK). Once purified 1µl of MDCC-SSB was added to 100µl of sample in a 96 well plate to make the final concentration 250nM. Alongside a control of MDCC-SSB alone, both the excitation and emission spectra were taken from 400nm-440nm and 455nm-550nm respectively. RT-PCR was undertaken using the Qiagen QuantiFast SYBR Green RT-PCR method, using primers as stated in the appendix, and unknowns were compared to samples of known quantities.

2.15 Real time transcription analysis.

Transcription was undertaken following the protocol and using the TranscriptAid T7 High Yield Transcription kit (Thermo scientific, Rochford, UK). The kits' control DNA, which produces a 2222nt long transcript, was used as the template for the analysis and 250nM MDCC-SSB was added to the transcription mixture. 0.25 μ M MDCC-SSB in the transcription buffer, 0.25 μ M MDCC-SSB and 0.25 μ M MDCC-SSB with 1 μ M ssDNA₇₀ both in 50mM Tris.HCl pH 7.5, 3mM MgCl₂ and 100mM NaCl, were all set as controls. The transcription ran for 3 hours at 37°C inside the ClarioStar microplate reader and emission at 470nm was measured in 1 minute intervals. A 1% agarose gel was used to analyse the products as instructed in the kits' protocol.

2.16 Circular Dichroism (CD) analysis.

Structures of the unlabelled SSB, MDCC-SSB, MDCC-SSB bound with ssDNA₇₀ and ssRNA₇₀ were all analysed at 0.2mg.mL⁻¹ in the far UV spectrum from 190nm-270nm using a Jasco J715 Circular Dichroism Spectrometer (Jasco Inc., Maryland, U.S.A). The proteins were incubated at 37°C and spectra were taken every 5 minutes for 3 hours. Following this incubation the samples were cooled down to 20°C and then heated up to 90°C with a measurement at 210nm being taken at 1°C intervals. 4 readings were taken for each measurement and averaged by the software provided. For the conversion of ellipticity to mean residue ellipticity the following equation was used (equation 3).

Equation 3)
$$[\theta]_{MRW} = \frac{\frac{MW}{(n-1)} \times \theta}{l \times c \times 10}$$

Where $[\theta]_{MRW}$ is the mean residue ellipticity, MW is the molecular weight of the protein, n is the number of amino acids, θ is the degrees in ellipticity, l is the path length in cm and c is the concentration in g.L⁻¹. Melting curves were established using Grafit (Erathicus, Horley, UK) and fitted with the sigmoidal Boltzman equation. The cuvette was made from quartz and had a pathlength of 0.1cm.

2.17 Dynamic light scattering analysis (DLS)

0.25 μ M of MDCC-SSB in 50mM Tris.HCl pH 7.5, 100mM NaCl, 3mM MgCl₂ in a 50 μ l cuvette was placed in a Zetasizer Nano ZS DLS machine (Malvern Instruments, Malvern, UK) under the guidance of a company representative. After 3 hours at 37°C the measurement was repeated. Analysis was undertaken using the Zetasizer software.

2.18 Photostability of MDCC

1 μ M of MDCC in 100 μ l of 50mM Tris.HCl pH 7.5, 100mM NaCl, 3mM MgCl₂ in a 96 well plate was incubated for 3 hours at 37°C. Fluorescence intensity was measured at 470nm every 5 minutes.

3. Results

3.1 Purification optimisation of G26c SSB.

3.1.1 Polymin P and Ammonium sulfate precipitation

The G26C SSB plasmid produced by Dillingham *et al.*, did not contain any purification tag. Cells containing the G26C SSB plasmid provided by Dillingham *et al* were defrosted and sonicated for 5 minutes overall. The protein purification protocol is from Dillingham *et al*⁴⁹. Briefly for protein purification the samples underwent a Polymin P (0.4%) precipitation alongside an ammonium sulfate (150g l⁻¹) precipitation. After final precipitation and centrifugation the pellet was resuspended in 50mL of 50mM Tris.HCl pH 8.3, 20% glycerol, 1mM EDTA and 0.2M NaCl. This resuspension was centrifuged at 18,000rpm for 20 minutes at 4°C and the supernatant was collected and kept at 4°C. A 5mL Heparin column (GE healthcare, Little Chalfont, UK) was equilibrated in 50mM Tris.HCl pH 8.3, 20% glycerol, 1mM EDTA and 50mM NaCl. The same buffer without NaCl was titrated into the supernatant to ensure the sample and column were at similar conductivities and the supernatant was loaded. The column was washed with the same equilibration buffer and eluted in a NaCl range of 50mM NaCl to 1M NaCl. The elutions were collected and analysed on an SDS-PAGE gel (figure 2.1) where little to no protein was present.

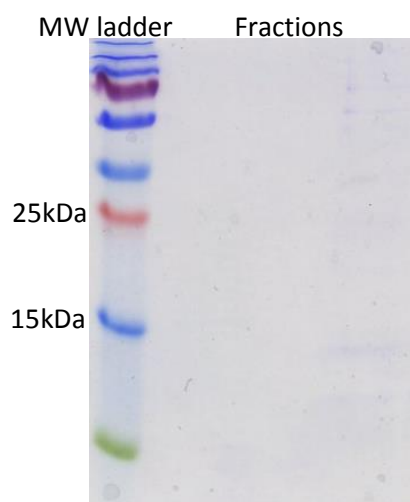


Figure 3.1. **SDS-PAGE analysis of Polymin P and ammonium sulfate precipitation method.** After both precipitations the sample was loaded onto a heparin column and eluted in 50mM Tris.HCl pH 8.3, 20% glycerol, 1mM EDTA and varied NaCl. No clear amount of protein in any elution fractions available for further use.

3.1.2 Heparin Column with a Gel Filtration column.

To ensure no loss of protein occurred the previous method was adapted. The same cells containing the same plasmid were defrosted and after cell sonication and centrifugation at 18,000rpm for 20 minutes at 4°C, the supernatant was collected and loaded onto a 5mL Heparin column (GE healthcare, Little Chalfont, UK) that had been equilibrated in 50mM Tris.HCl pH 8.3, 20% glycerol, 1mM EDTA and 50mM NaCl. After washing once with the equilibration buffer the column was eluted using the same buffer with a NaCl range from 50mM to 1M NaCl. The sample was then analysed on SDS-PAGE (figure 2.2a) Defined bands were shown at the molecular weight of single SSB subunits of approximately 18,890kDa the theoretical mass of each SSB subunit. Samples containing SSB were then loaded onto a Superdex 200 10/300 GL gel filtration column (GE healthcare, Little Chalfont, UK) which was equilibrated in 50mM Tris.HCl pH 7.5, 1mM DTT, 150mM NaCl. The column was washed and eluted in this buffer. The samples were collected and analysed using SDS-PAGE (figure 2.2b). Whilst this method led to SSB elution the samples were deemed to be of too small amounts and too impure.

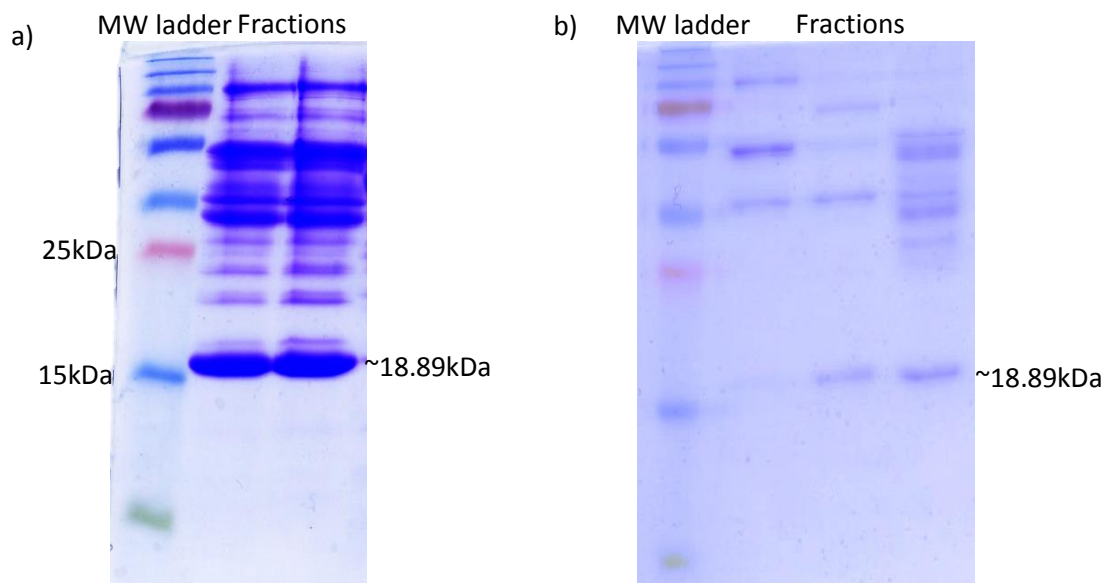


Figure 3.2. **SDS-PAGE of heparin column and gel filtration column method.** a) Presence of over expressed SSB after heparin column elution in 50mM Tris.HCl pH 8.3, 20% glycerol, 1mM EDTA. The two elution fractions were pooled together and loaded onto a gel filtration column in 50mM Tris.HCl pH 7.5, 1mM DTT, 150mM NaCl. The elutions were analysed using SDS-PAGE (b) which showed presence of SSB in small impure quantities.

3.1.3. Ammonium sulphate precipitation with a Q sepharose column.

This method was adapted from Green *et al*⁶³. Briefly, after cells containing the unlabelled SSB plasmid were defrosted, sonicated and centrifuged at 18,000rpm for 20 minutes at 4°C, the supernatant was collected and 20% w/v ammonium sulphate was added and followed by a subsequent centrifugation at 18,000rpm at 4°C forced precipitation. The pellet was resuspended in 20mM Tris pH 7.5, 20mM NaCl and loaded onto a 5mL HiTrap Q column (GE healthcare, Little Chalfont, UK). Elution occurred over 0-1M NaCl gradient. Those elutions were analysed using SDS-PAGE (figure 2.3a) and those containing protein were pooled and loaded onto a Superdex 200 10/300 GL gel filtration column (GE healthcare, Little Chalfont, UK) which was equilibrated in 50mM Tris.HCl pH 7.5, 1mM DTT, 150mM NaCl. The column was washed and eluted in this buffer. The samples were collected and analysed using SDS-PAGE (figure 2.3b).

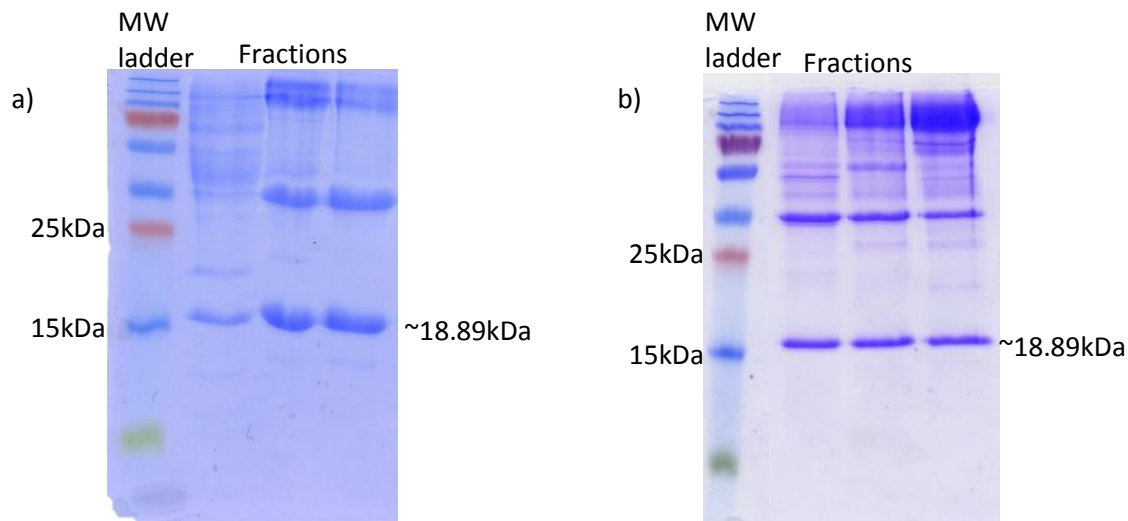


Figure 3.3. **SDS-PAGE analysis of the adaptation of the Green *et al*⁶³ SSB purification method.** a) 3 elutions from the Q sepharose column were analysed using SDS-PAGE, they show the presence of SSB with some contaminants. After pooling of the elutions they were loaded onto a gel filtration column. Three elutions fractions were collected and analysed using SDS-PAGE. Protein was present in all fractions however the analyses showed potential contaminants.

3.1.4 His-tagged SSB

E. coli cells containing the His-tagged SSB PET151 plasmid, were defrosted, sonicated for 5 minutes and centrifuged at 18,000rpm at 4°C. The supernatant was then collected and stored at 4°C. A 5mL His-Trap HP column (GE healthcare, Little Chalfont, UK) was equilibrated in 50mM Tris.HCl pH 7.5, 40mM imidazole, 500mM NaCl and 1mM DTT. The supernatant was loaded onto the column and the column was washed with the equilibration buffer. The buffer was eluted using the same buffer with increasing imidazole concentrations from 40mM to 400mM. Samples were collected and analysed using SDS-PAGE (figure 2.4).

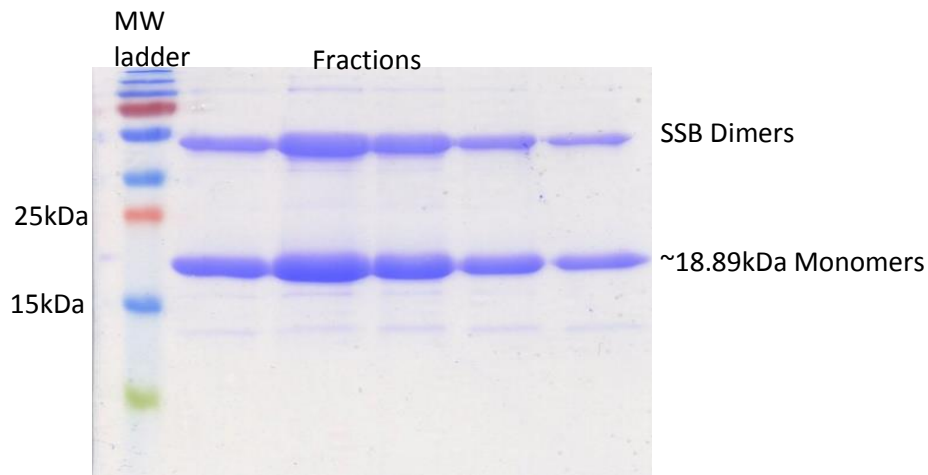


Figure 3.4. **An SDS-PAGE gel showing the presence of SSB.** Targeted elution fractions from the His column that have the presence of SSB both in its monomer and dimer form in 50mM Tris.HCl pH 7.5, 500mM NaCl and 1mM DTT and unknown imidazole concentration.

3.2 Proving SSB does bind to mRNA.

Fluorescent and non-fluorescent techniques show that SSB is a viable scaffold for an mRNA biosensor, as it binds to mRNA as previously shown⁶¹. Electrophoretic mobility shift assay (EMSA) shows that purified SSB is functional and is able to bind to ssRNA₇₀ in a similar way to that of ssDNA at low NaCl concentrations (figure 3.1). Due to a lower concentration of protein compared to substrate it was not expected to get complete shift of all substrate.

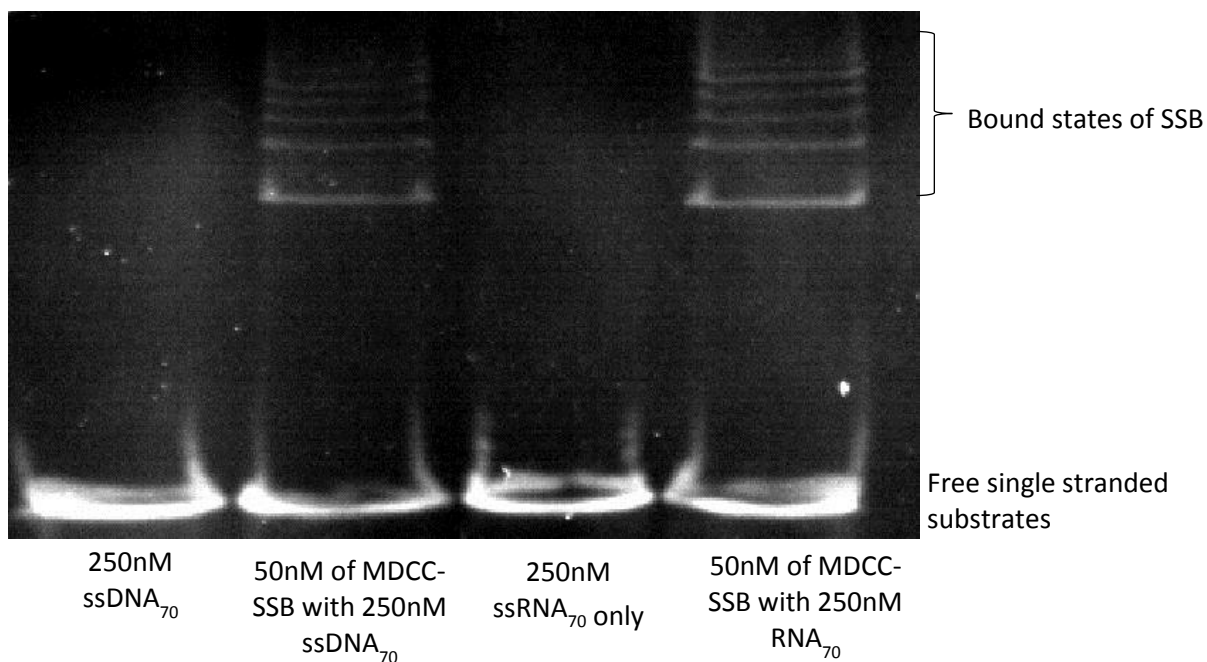


Figure 3.5. **EMSA of SSB bound to both ssDNA₇₀ and ssRNA₇₀.** 50nM of MDD-SSB was incubated with 250nM ssDNA₇₀ or ssRNA₇₀ for 20 minutes at room temperature in a 100mM NaCl buffer and analysed using 12% acrylamide gel stained with SYBR®Gold. The unbound substrates progressed further through the gel to that of the bound. Both the bound ssDNA₇₀ and ssRNA₇₀ have similar splitting of bands.

This EMSA showed similar binding properties for both substrates. To further confirm SSB does bind to ssRNA and to define the kinetic parameters, tryptophan fluorescence studies were used. Tryptophan reports on the intrinsic protein fluorescence. This type of fluorescence reflects the local environment the tryptophan residues are found in, and so when binding occurs, these microenvironments change due to SSB changing its conformation. In SSB four tryptophan residues can be found at positions; 41, 55, 89 and 136. It has been shown that the tryptophan at position 54 is involved directly in the binding of ssDNA⁶⁴. Tryptophan fluorescence was measured in two salt concentrations using two different methods. At 100mM NaCl, tryptophan fluorescence was measured using a fluorescence spectrophotometer. Previously Lohman *et al*⁶⁵ have observed 80% fluorescence quenching when SSB

was bound to ssDNA at a higher salt concentration⁶⁶. The second method employed to measure tryptophan fluorescence at a high salt concentration was to use thermophoresis, where serial dilutions within small capillaries were set up to measure the intrinsic fluorescence measured with a label free NanoTemper machine (NanoTemper technologies, Munich, Germany).

As shown in figure 3.2 at 100mM NaCl, saturation of the tryptophan quenching when using 50nM SSB occurs at 25nM ssDNA₇₀. The results were fitted using two linear regressions to identify a point in which tryptophan quenching reaches a maximum and an increase of substrate does not cause further tryptophan quenching. This tight binding of ssDNA₇₀ result implies that at low salt, there is one SSB tetramer binding to two molecules of ssDNA₇₀. When SSB binds to increasing concentrations of the RNA substrate, ssRNA₇₀, saturation of the tryptophan quenching occurs slightly higher at 34nM. This implies there is at least a 1:1 binding ratio of SSB to ssRNA₇₀ molecules but potentially there could be two. However the data quality is not ideal with multiple outliers, and so to make an accurate judgement further work is required. Whilst it is difficult to predict the SSB species this study has shown that binding to both substrates behaves in a similar manner at low salt concentrations. One factor that needs to be taken into consideration is that DNA substrates are also able to emit some fluorescence at 325nm and so can provide background fluorescence which limits signal quenching and so 100% tryptophan quenching cannot be seen to occur.

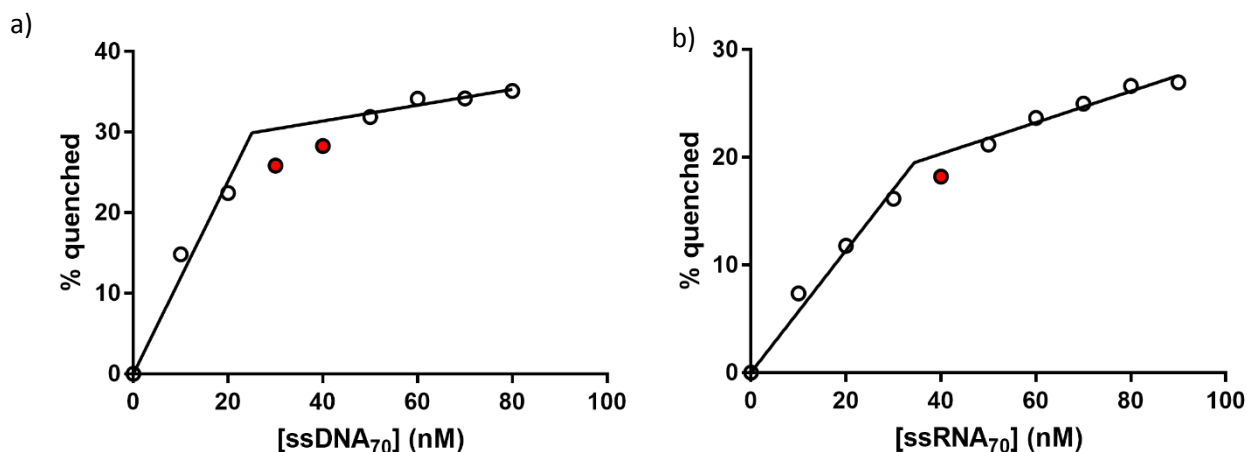


Figure 3.6. **Tryptophan quenching shows similar binding of ssDNA₇₀ and ssRNA₇₀ substrates to SSB.**

In 100mM NaCl buffer, 50nM SSB was titrated with ssDNA₇₀ (a) or ssRNA₇₀ (b) and the intrinsic tryptophan fluorescence quenching was measured at 325nm. The intensities were corrected for dilution and quenching saturation was measured to occur at 25nM and 34nM respectively. This was calculated from the interception of the two linear regression fits and both results show a stoichiometry of 1:1. Outliers of the linear regressions are highlighted in red.

A second method to study binding was to use thermophoresis. Microscale thermophoresis uses infrared light to slightly increase the temperature of a specific area⁶⁷. Tryptophan fluorescence is measured after irradiation to quantify changes in the mobility of the protein, since protein bound to substrate would have a reduced mobility compared to its free form. ssDNA₇₀ and ssRNA₇₀ titrations were completed at a higher salt concentration in PBS buffer to further characterise mRNA binding. Using intrinsic tryptophan fluorescence, the Label Free NanoTemper was used to observe tryptophan fluorescence across a serial dilution of ssDNA₇₀ and ssRNA₇₀ substrates. Concentrations of ssDNA₇₀ and ssRNA₇₀ (0-1 μ M) were titrated against 50nM of SSB and the tryptophan quenching was calculated with the software provided. The observed apparent K_d 's are 50nM and 164nM respectively. This shows that at a higher salt concentration the binding stoichiometry of SSB to ssDNA₇₀ is once again 1:1, but due to the higher value for observed apparent K_d with ssRNA₇₀ binding, this could correspond to SSB

subunits binding in a dimeric form to the ssRNA₇₀. Therefore a stoichiometry of $[SSB_{monomers}]_2: 1$ ssRNA₇₀ is observed. The results were plotted as shown in figure 3.3 and provided by NanoTemper (Munich, Germany). This result shows a difference in binding strength but still confirms SSB's ability to bind to mRNA.

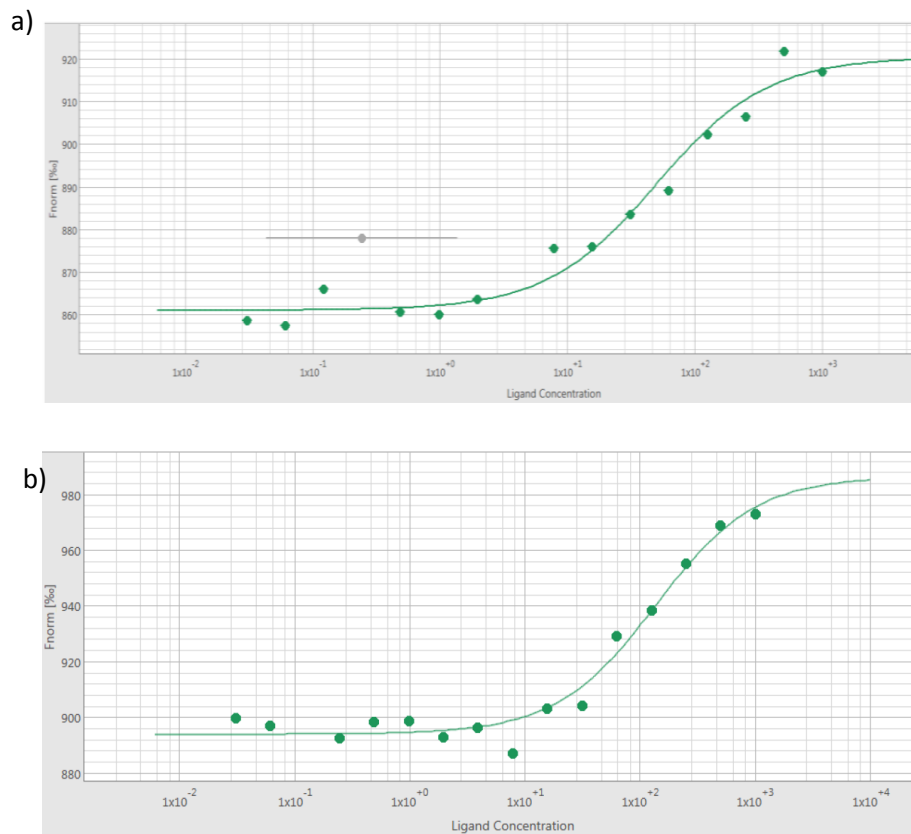


Figure 3.7. **SSB's Intrinsic Tryptophan fluorescence movement measured by the label free NanoTemper.** 50nM of SSB in 1x PBS buffer was kept constant whilst (a) ssDNA₇₀ or (b) ssRNA₇₀ concentrations varied between 10 μ M- 30pM. The assay was performed in PBS with 0.05% TWEEN-20. After short incubation samples were loaded into MST NT.Labelfree standard glass capillaries and the tryptophan fluorescence was analysed. Concentrations on the x-axis are plotted in nM. For ssDNA₇₀ the observed K_d is measured to be 50nM with one outlier and ssRNA₇₀ K_d observed to be 134nM.

A fluorescent method reinforces that SSB binding to mRNA does occur. SSB was titrated against fluorescein (f) labelled nucleotides, fssDNA₁₆ and fpolyU₂₀ (figure 3.4). Upon addition of SSB to these fluorescent substrates, quenching of the fluorescent signal is observed. Whilst fluorescent quenching occurred, there was no clear concentration dependent binding curves for either substrates. The amount of fluorescence quenched decreased over SSB concentration for ssDNA₁₆ but when titrating into polyU₂₀ a binding curve is not apparent. There also seems to be clear outliers at 1 μ M SSB for both fluorescent nucleotide substrates. These final SSB binding results support the previous data shown and corroborates the previous statement that SSB does bind to ssRNA₇₀.

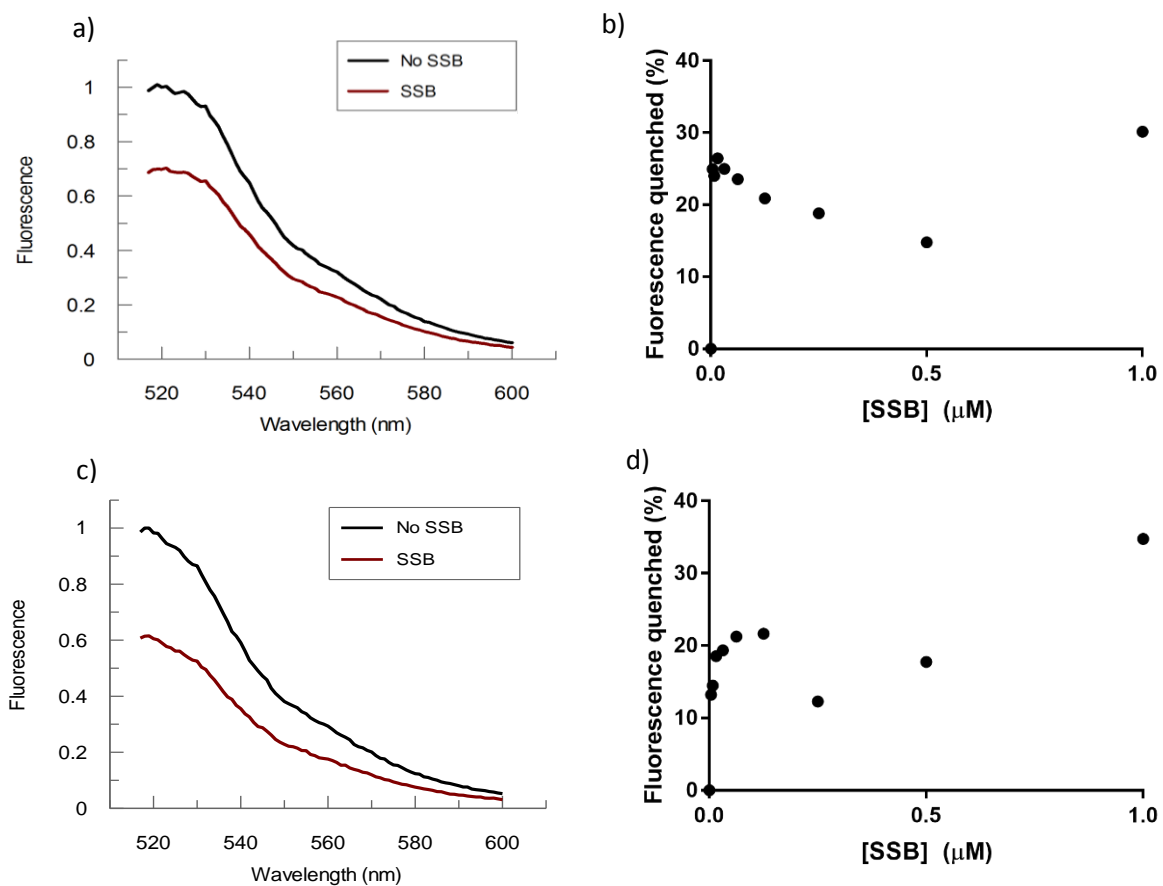


Figure 3.8. **Quenching of fluorescein nucleotides due to SSB titrations.** 1 μ M SSB was titrated into 1 μ M of fssDNA₁₆ (a,b) and 1 μ M of fpolyU₂₀ (c,d) in 100mM NaCl buffer. Complete emission scans were taken from 520nm to 600nm with and without 1 μ M SSB and normalised to 1 (a,c). Fluorescence quenched against SSB concentration was taken from the fixed wavelength of 520nm (b,d).

To confirm the weaker binding of SSB to ssRNA compared to ssDNA, as observed in previous results, a competition assay was set up using fluorescein labelled ssDNA₄₀ (fssDNA₄₀) (figure 3.5). In this assay, alongside two controls of bound SSB-fssDNA₄₀ and free fssDNA₄₀, SSB was pre-incubated with 1 μ M of ssRNA₇₀ and the emission spectra were taken from 520-600nm. fssDNA₄₀ was added and the spectra were retaken. These spectra matched that of the SSB bound to fssDNA₄₀ and not the free fssDNA₄₀ which implies the ssRNA has been outcompeted by the fssDNA₄₀. This shows that SSB has weaker binding to ssRNA and potentially has preferred affinity to ssDNA. This could be explained by non-specific interactions between the protein and the fluorophore. Moreover due to the two different binding modes of SSB it could be possible that both fssDNA₄₀ and ssRNA₇₀ are bound in tandem with two OB-folds binding to each substrate. To improve the competition assay fssDNA₇₀ substrates should be used, however, their cost and low yield of production is a limiting factor.

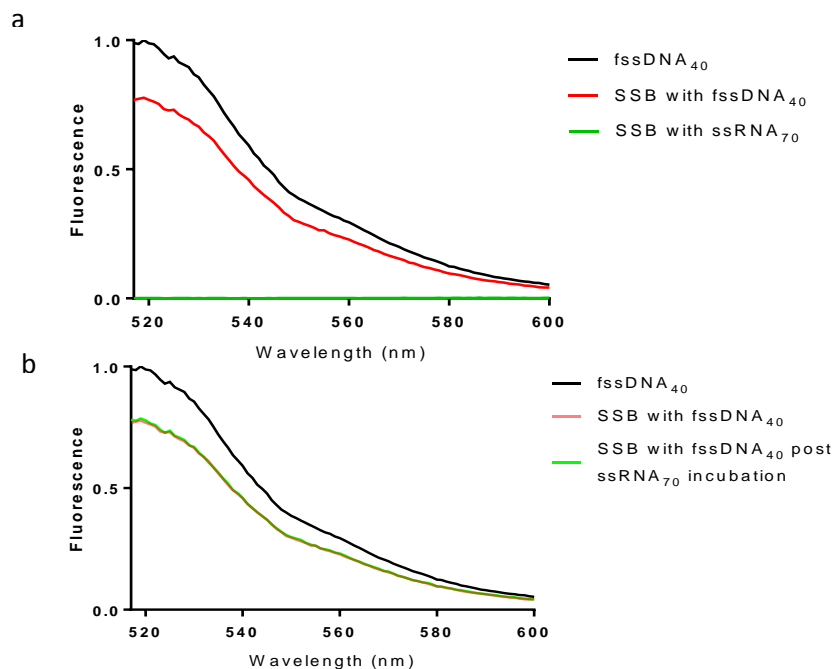


Figure 3.9. **fssDNA₄₀ outcompetes ssRNA₇₀ for SSB binding.** 75nM SSB was incubated with 1 μ M ssRNA₇₀ along with two controls, 50nM fluorescein ssDNA₄₀ (fssDNA₄₀) and 50nM fssDNA₄₀ with 75nM SSB. After emission spectra (520-600nm) were taken, 50nM of fssDNA₄₀ was added to the SSB, ssRNA₇₀ mixture and the emission was re-measured. All spectra were normalised to 1. The fluorescence spectra show the same fluorescence as the SSB with fssDNA₄₀ solution showing binding of fssDNA₄₀ has occurred and the ssRNA₇₀ has been displaced.

3.3 The design of the MDCC-SSB biosensor.

The point mutation of glycine to cysteine at position 26 provides the only cysteine residue within the protein, which limits the side effects of fluorescent labelling such as over labelling. SSB labelling optimisation was able to be carried out due to this single cysteine residue, ensuring the highest amount of SSB monomers were labelled with MDCC. Incubation lengths and temperatures were as shown in table 1. Four hours incubation with MDCC at room temperature is the optimum labelling condition. In its tetrameric formation this leads to 3 out of 4 subunits to be fluorescently labelled. Whilst similar labelling is observed over night at 4°C, to make labelling quick and easy it is recommended to incubate SSB with MDCC for a minimum of 4 hours. Appropriate molecular weights were observed for both MDCC-SSB and unlabelled SSB using SDS-PAGE analysis (figure 3.6).

Length of Time	Concentration of SSB monomers (μM)	Concentration of MDCC (μM)	Amount of monomers labelled in a tetramer.
2 Hours	1 μM	0.4 μM	$\sim 1/2$
4 Hours	16.6 μM	13.2 μM	$\sim 3/4$
Overnight at 4°C	14.1 μM	10.7 μM	3/4

Table 1. **Table to show optimisation of MDCC labelling of SSB.** Optimised labelling occurs after 4 hours at room temperature. Incubation times varied from 2 hours to overnight. The concentrations of SSB monomers were measured at 280nm with extinction coefficient of 25,000 $\text{cm}^{-1} \text{M}^{-1}$ and MDCC concentrations were measured at 435nm with extinction coefficient of 50,000 $\text{cm}^{-1} \text{M}^{-1}$. A ratio of the concentrations was taken.

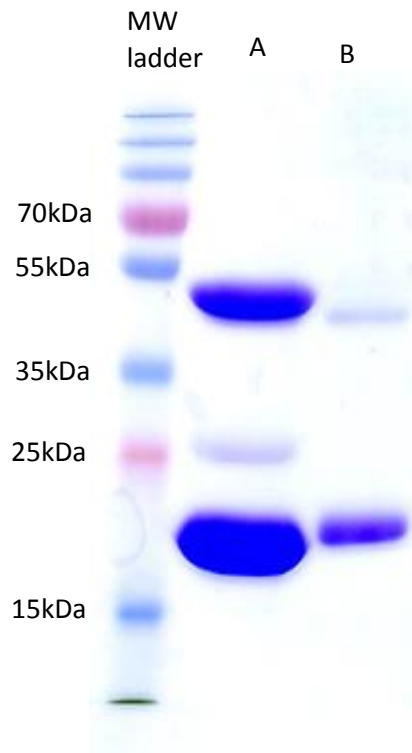


Figure 3.10. **SDS-PAGE gel showing labelling of SSB with MDCC-SSB.** Both samples of SSB (A) and MDCC-SSB (B) were analysed using SDS-PAGE. (A) Showed a large band at approximately 18.9kDa and 37.8kDa which are SSB subunits as monomers and dimers. (B) shows a band at 19.27kDa which is MDCC labelled SSB monomers due to DTT treatment and a slight band at approximately 37kDa showing unlabelled dimers remaining after the DTT treatment.

A sufficient signal was ensured by measuring the fluorescence intensity using a serial dilution of SSB subunits from $1\mu\text{M}$ - $0.0625\mu\text{M}$ (figure 3.7). The fluorescence signal is MDCC-SSB concentration dependent and occurs in a linear fashion at both 100mM NaCl and 200mM NaCl concentrations. This shows that there are no artificial signals from the wells used in the plate reader and the protein and signal are stable over varying concentrations. 200nM subunits, 50nM SSB tetramer was deemed a suitable concentration to produce a reliable signal for further studies- the biosensor had the potential at higher concentrations to form oligomers which would affect the signal, or at lower concentrations the tetramer could have dissociated, forming monomers and leading to unpredictable changes in

signal. However, this was seen to not be the case. When MDCC is bound to SSB its excitation peak occurs at 435nm and the emission peak is at 470nm, giving a Stokes shift of 35nm.

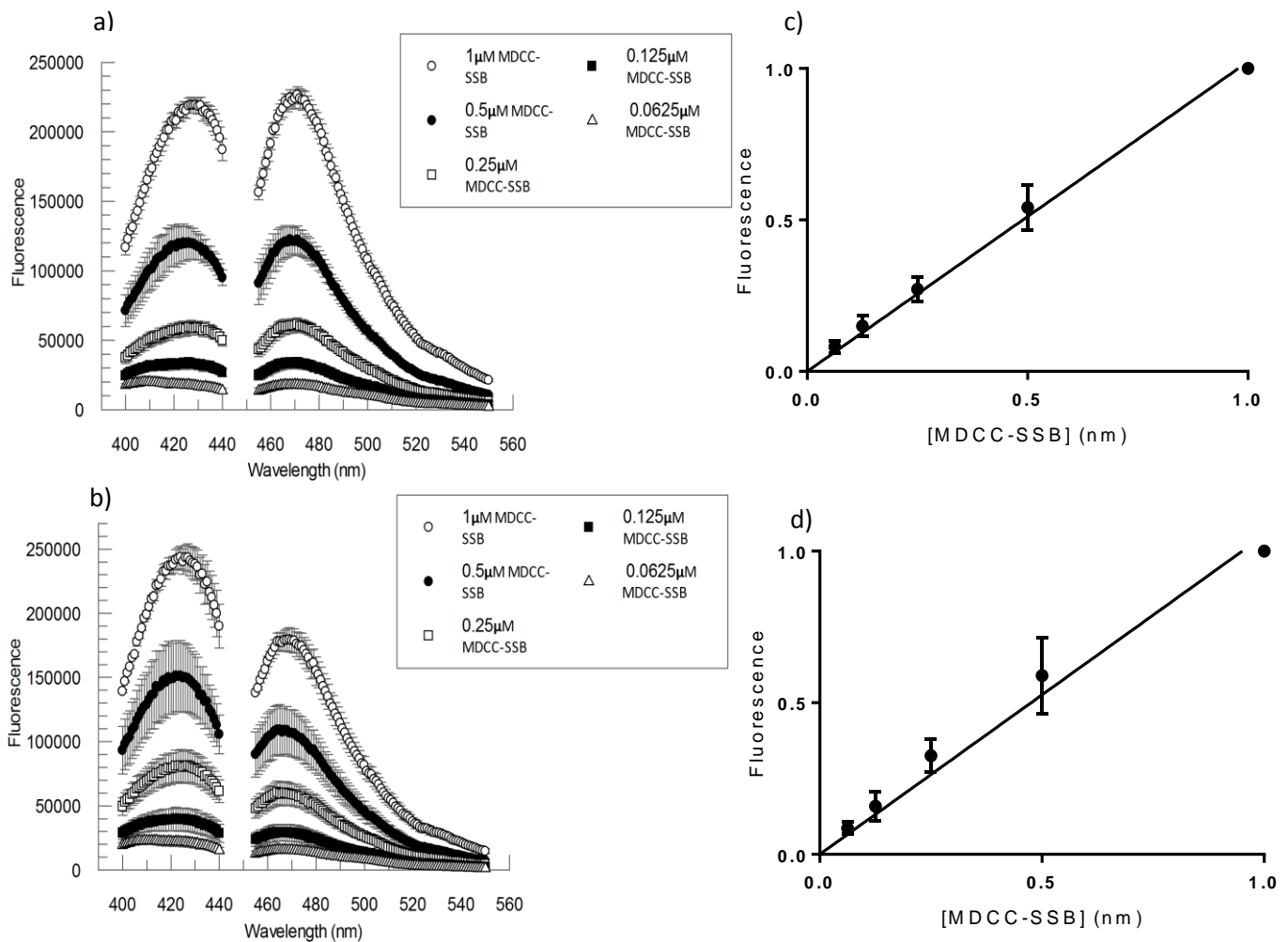


Figure 3.11. Fluorescence increases in a linear fashion with increasing MDCC-SSB subunits at both high and low salt conditions. MDCC-SSB was serially diluted from 1 μM to 0.0625 μM and was made up to 100 μl in 100mM (a) or 200mM (b) NaCl buffer in a 96 well plate. Excitation spectra were taken from 400-440nm and emission fluorescence taken from 455-550nm. Excitation peak occurred at 435nm and emission peak at 470nm with a Stokes shift of 35nm. 3 spectra were averaged and plotted with standard error for each concentration. Emission measured at 470nm was normalised to 1 and plotted against MDCC-SSB subunit concentration in 100mM NaCl buffer (c) and 200mM NaCl buffer (d) with standard deviation, showing a linear increase with a signal being stable at high and low salt concentrations.

The biosensor responds to the addition of ssRNA and ssDNA substrates. A 1.9 fold increase is observed when $1\mu\text{M}$ of ssDNA₇₀ is added to 50nM MDCC-SSB tetramers and a 2.1 fold increase is observed with addition of $1\mu\text{M}$ ssRNA₇₀ to 50nM MDCC-SSB tetramers (figure 3.8). This corroborates with previous studies^{49,63} that a fluorescence increase is observed when SSB with a coumarin dye attached binds to ssDNA₇₀. It also shows MDCC-SSB is a suitable biosensor for ssRNA detection. The Stokes shift for both substrates and the MDCC-SSB alone remains the same at 35nm.

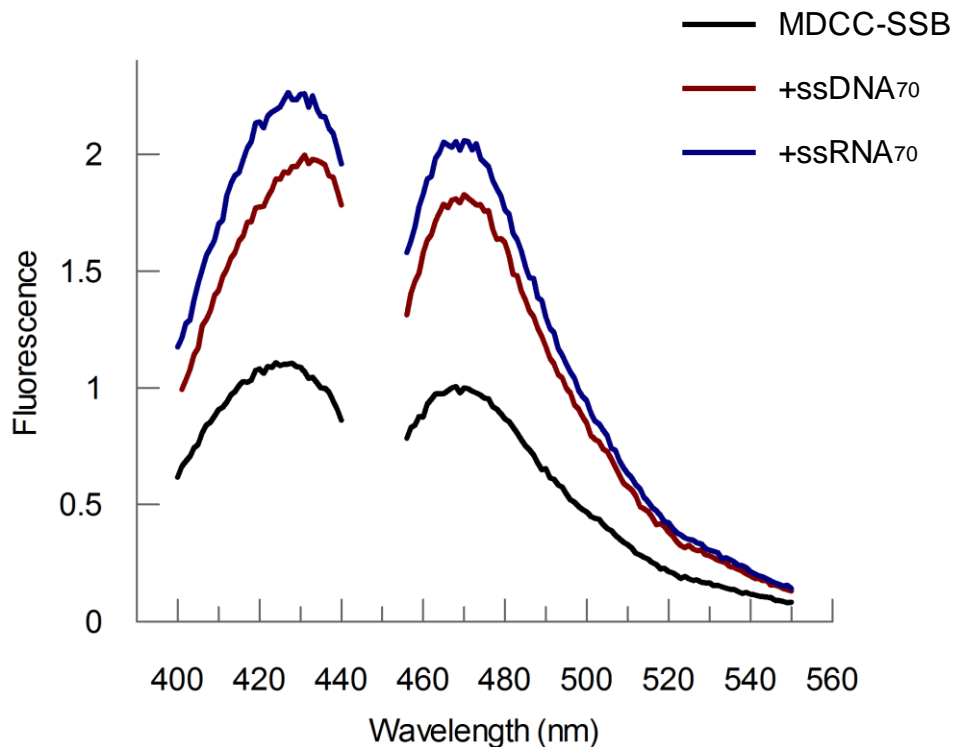


Figure 3.12. **Excitation and emission scan of MDCC-SSB with and without substrates.** 50nM MDCC-SSB tetramers were incubated with $1\mu\text{M}$ of ssDNA₇₀ or $1\mu\text{M}$ ssRNA₇₀ in 100mM NaCl buffer. Compared to MDCC-SSB alone there was a 1.9 fold increase in fluorescence when bound to ssDNA₇₀ and 2.1 fold increase when bound to ssRNA₇₀. Excitation spectra was taken from 400-440nm and emission was taken from 455-550nm.

3.4 Testing the biosensor

As shown previously by Dillingham *et al.*,⁴⁹ the MDCC-SSB can be used to measure helicase activity. To ensure the biosensor designed here behaves in a similar way, the helicase PcrA activity was measured in real time. A 1000 base pair linear dsDNA fragment was incubated with the helicase

loading factor, RepD. Once incubation was complete, helicase activity was initiated with the addition of PcrA and ATP. Following a lag phase which is typical for PcrA⁶⁸, a fluorescence increase was observed over 2.5 minutes in real time as the dsDNA is unwound and MDCC-SSB binds to the available ssDNA. The signal then reached a plateau as the unwinding was complete (figure 3.9). With the concentration of DNA being 1000 base pairs long there are 15 potential binding sites for (SSB)₆₅. This means the concentration of binding sites of 5nM DNA substrate is 75nM. The peak fluorescence increase shown in this study has seen to be 1.9 fold for ssDNA when saturating the biosensor. In this assay though there was only a fluorescent increase 10% of this figure. This suggests that dsDNA was not completely unwound, as saturation of the sensor should have occurred at 50nM of biosensor. Incomplete unwinding could be due to damaged RepD within the sample, as helicase activity will not occur without RepD loading PcrA, inhibiting normal helicase binding to the dsDNA.

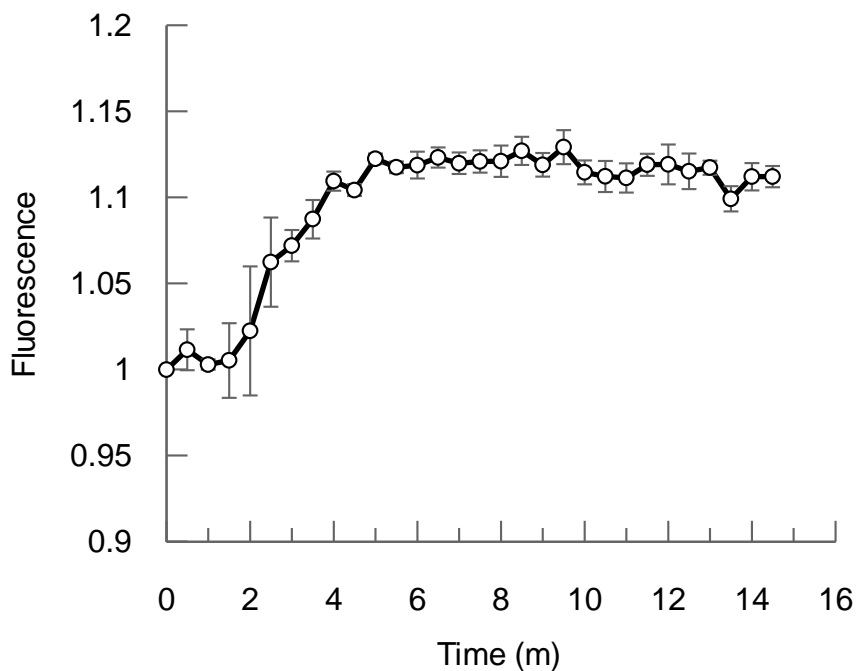


Figure 3.13. **Fluorescence increase as MDCC-SSB binds ssDNA produced by the helicase PcrA.** 5nM 1kbp dsDNA was incubated with 20nM RepD and 50nM MDCC-SSB tetramers at 30°C for 15 minutes. After incubation 100nM PcrA and 1mM ATP was added initiating the reaction which was allowed to proceed for 15 minutes at 30°C in 100µl in a 96 well plate in a micro plate reader. Fluorescence was measured at 470nm.

3.5 Characterisation of the MDCC-SSB biosensor

All quoted concentrations for MDCC-SSB within this section refer to the concentration of MDCC-SSB tetramers unless stated otherwise. MDCC-SSB fluorescence increase is dependent on the concentration of ssDNA₇₀. Until a saturation point, there is a linear increase in fluorescence that can be used to calibrate the biosensor. SSB is a tight binding protein, as a result, the interaction with ssDNA has a small K_d (within the low pM to low nM range)⁶⁹, therefore any free ssDNA should be bound by the biosensor. This, however, means that when using lower MDCC-SSB concentrations the DNA may not be detected before the K_d is approached. This tight binding theoretically means that a fluorescence signal should increase linearly up to the MDCC-SSB concentration used. Once this has been reached, a plateau should occur depending on the SSB species within the sample. This has been explained in figure 3.10.

When titrating ssDNA₇₀ into MDCC-SSB solution there is a clear linear phase in both 100mM NaCl and 200mM NaCl buffers however the saturation points observed are not identical (figure 3.11). At 100mM NaCl, saturation of the sensor occurred at 64.3nM which means at a concentration of 50nM, MDCC-SSB is able to distinguish between ssDNA₇₀ concentrations of 3.9nM, the lowest titre, to 104.4nM. At 200mM NaCl saturation of the sensor occurs earlier at 90.3nM, which is only a slight reduction in sensitivity of MDCC-SSB. The later saturations are most likely due to a mixture of labelled tetramers and dimers as well as unlabelled species. During the titrations there are some strong outliers that do not fit the linear regressions, therefore, care has to be taken when using this sensor as the results may not always be clear to compare the fluorescence intensity to a substrate concentration.

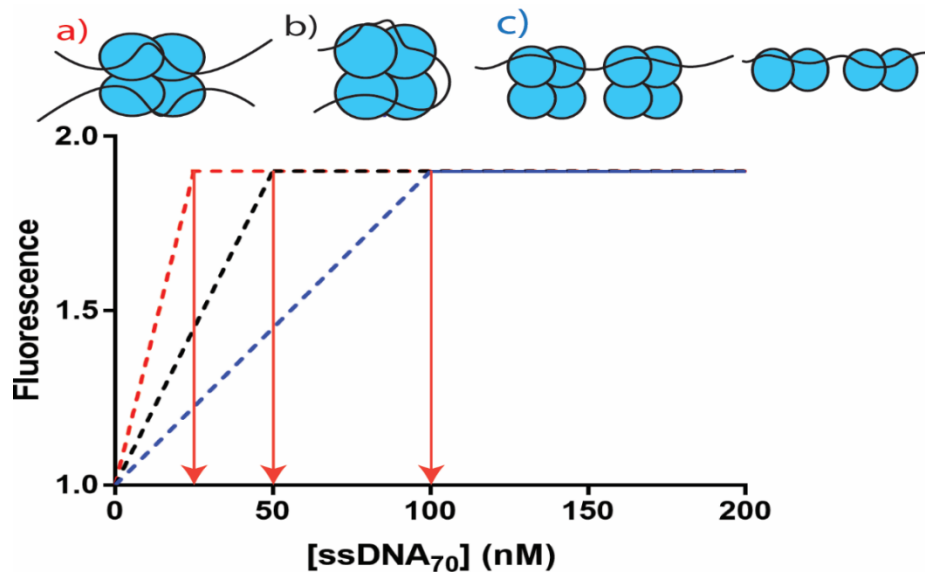


Figure 3.14. **Potential binding modes of 50nM MDCC-SSB with the titration of ssDNA₇₀ substrates, showing a variation in fluorescence saturation.** Due to the low K_d of SSB it is expected that binding occurs rapidly within the MDCC-SSB system. From this, it is assumed that if 50nM MDCC-SSB is used, at the point of signal saturation all MDCC-SSB proteins are bound to substrate. Therefore if a saturation point occurs at 25nM ssDNA₇₀ (a) then all MDCC-SSB tetramers are bound to two substrates each. If saturation occurs at 50nM ssDNA₇₀ (b) then a 1:1 stoichiometry occurs in which there is one ssDNA₇₀ to one SSB tetramer. If a saturation is observed at 100nM ssDNA₇₀ then there could be two potential binding modes of SSB in which two tetramers bind along the ssDNA₇₀ in a (SSB)₃₅ binding mode or two dimers bind along the ssDNA₇₀ in a similar manner (c).

MDCC-SSB fluorescence increase also occurs with an increase in ssRNA₇₀ concentration, similar to that shown with ssDNA₇₀. A linear phase occurs at both high and low salt and the saturation point for ssRNA₇₀ occurs later compared to that seen with ssDNA₇₀ (figure 3.12). At low salt concentrations a saturation point occurred at 101nM of ssRNA₇₀ and at the higher salt concentration a saturation point occurs at 109nM, as shown in figure 3.3.3. This shows the biosensor has an increased sensitivity to

ssRNA₇₀ compared to ssDNA₇₀ in both salt concentrations as it is able to distinguish concentrations from the 3.9nM titre to 109nM ssRNA .

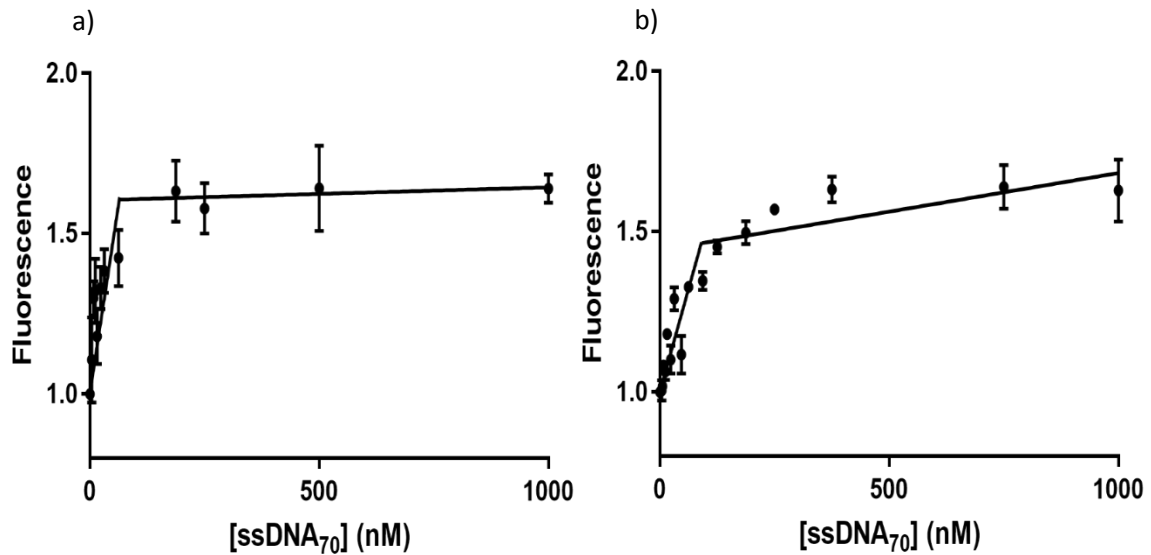


Figure 3.15. **Titrations of ssDNA₇₀ with 50nM MDCC-SSB showing a linear phase and a saturation phase.** ssDNA₇₀ was serially diluted against 50nM of MDCC-SSB and the fluorescence emission was measured at 470nm in a 96 well plate. The increase was normalised to MDCC-SSB alone and corrected for dilutions, then plotted with standard error. The titrations were done in 100mM NaCl buffer (a) where a saturation was seen at 64.3nM of ssDNA₇₀ or 200mM NaCl buffer (b) where a saturation of sensor was seen at 90.3nM ssDNA₇₀. Both titrations showed a linear phase but saturated at a later point than expected.

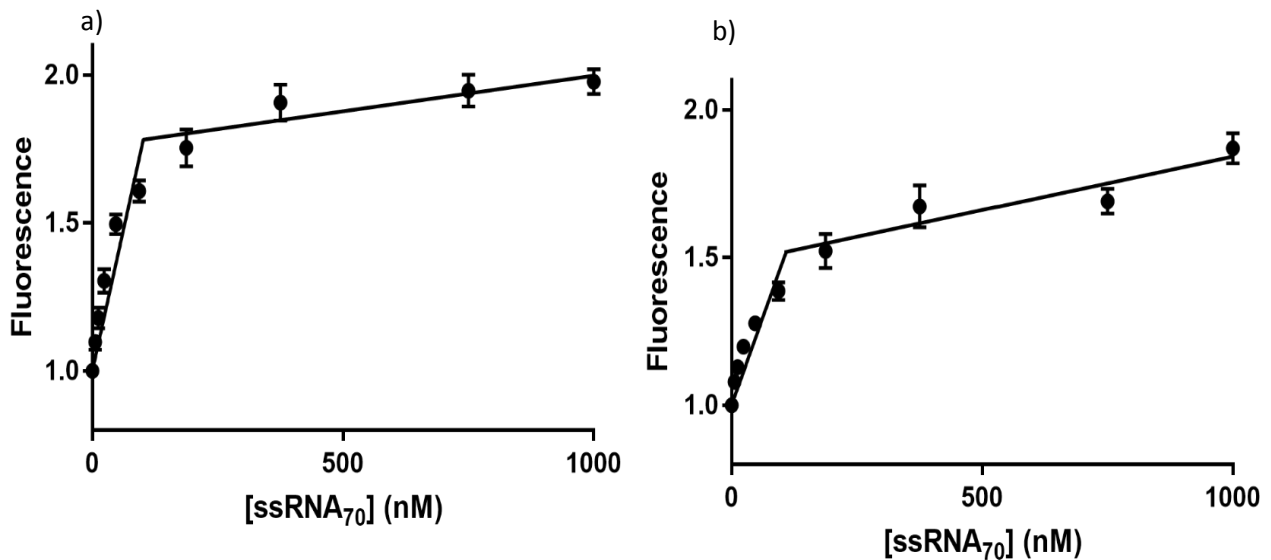


Figure 3.16. Titrations of ssRNA₇₀ with 50nM MDCC-SSB showing a two phase system. ssRNA₇₀ was serially diluted against 50nM of MDCC-SSB and the fluorescence emission was measured at 470nm in a 96 well plate. The increase was corrected for dilution and normalised to MDCC-SSB alone, then plotted with standard error. The titrations were done in 100mM NaCl buffer (a) with saturation observed at 101nM of ssRNA₇₀ or 200mM NaCl buffer (b) where saturation of the sensor was observed at 109nM ssRNA₇₀. At both high and low salt concentrations, a linear phase was observed.

3.6 Application of MDCC-SSB biosensor to measure *in vitro* transcripts.

The biosensor has shown its ability to bind to ssRNA and the fluorescence signal corresponds to concentrations of ssRNA present. To test the capability of the biosensor to detect concentrations of mRNA samples of different lengths other than the 70 nucleotide long samples previously used, an *in vitro* transcription assay was set up. The template DNA was the gene RecD2 with a T7 promotor which results in a 2225 nt run off. The transcription assays were set to run for varying amounts of time resulting in different mRNA concentrations. Once the mRNA was purified, it was quantified using RT-qPCR. Quantification was performed against a series of known amounts of template. The amount of mRNA assumes complete transcription of the 2225 nucleotides. This is likely to be viable to due

abortive transcriptions that will not be able to bind to the PCR primers. 1 μ M of MDCC-SSB was added to each sample of purified mRNA and the excitation and emission spectra were taken and compared to the RT-qPCR results. MDCC-SSB can be used qualitatively to compare mRNA transcripts present and there is a linear increase in fluorescence compared to amount of mRNA transcript (ng) (figure 3.13). This linearity shows the biosensor can be used quantitatively.

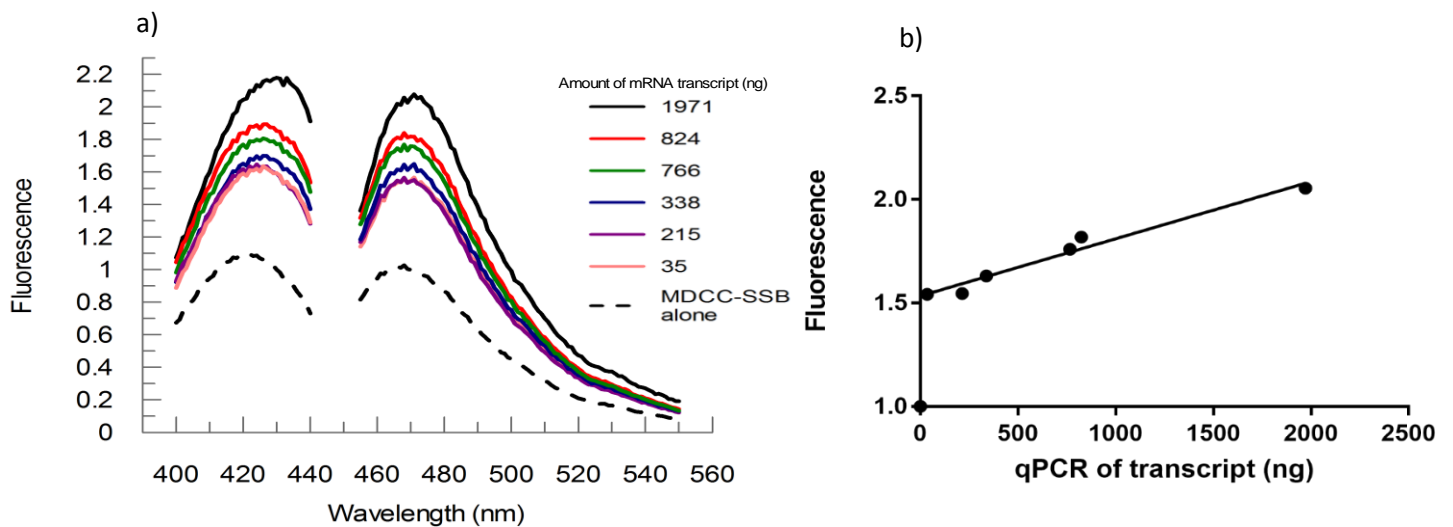


Figure 3.17. **MDCC-SSB biosensor can be used to compare transcription samples.** 1 μ M was added to pure mRNA transcripts produced by the T7 polymerase transcribing a 2225nt transcript for various lengths of time resulting in different amounts (ng) of mRNA. The excitation (400-445nm) and emission (450-550nm) spectra were taken of each sample with MDCC-SSB alone as the control (a). RT-qPCR of the samples were performed against known amounts of template and the amounts of mRNA transcribed were calculated from this. Peak emission of the MDCC-SSB at 470nm was then plotted against the amount of mRNA transcript calculated using RT-qPCR (b). There is a clear linear increase in fluorescence, which is dependent on the amount of mRNA transcribed. The MDCC-SSB fluorescence reflected the difference in mRNA concentrations.

The qualitative study showed that MDCC-SSB does respond to the different concentrations of nucleotides. However, with the lowest amount of mRNA transcribed being 35ng and the next being 215ng there is some overlap in the low concentration MDCC-SSB fluorescence spectra (figure 3.13a).

This result could be due to contaminated samples containing ssDNA or errors in the calculated mRNA amounts. The final assay was to undertake a T7 polymerase transcription whilst MDCC-SSB is present in the solution, and to observe the transcription of mRNA in real time by measuring the fluorescence emission of the MDCC-SSB.

MDCC-SSB is not a suitable biosensor for the real time measurement of transcription due to a loss of fluorescence over time (figure 3.14). In this assay the T7 polymerase kit was used to transcribe a DNA template of 2223nt with 250nM of MDCC-SSB incorporated into the assay. A few controls were set up, including MDCC-SSB in the transcription buffer only; MDCC-SSB in the 100mM NaCl buffer, as previously used, and MDCC-SSB with ssDNA₇₀ in the 100mM NaCl buffer. This allowed any changes of fluorescence over time in the transcription buffer to be solely down to the transcription of mRNA. As the assay ran, a decrease in fluorescence occurred in all controls and the transcription assay. The decrease in fluorescence occurred more dramatically in samples that contained either mRNA or ssDNA₇₀, with the MDCC-SSB alone in 100mM NaCl buffer losing the least amount of fluorescence. The decrease occurred in a clear rapid phase over ten minutes and then decreased at a steady rate for the remainder of the assay.

To ensure mRNA was being transcribed by the T7 polymerase and the biosensor was not responding, gel electrophoresis was used to show the presence of mRNA. The transcription sample was run on a 1% agarose gel and stained with SYBR Gold (figure 3.15).

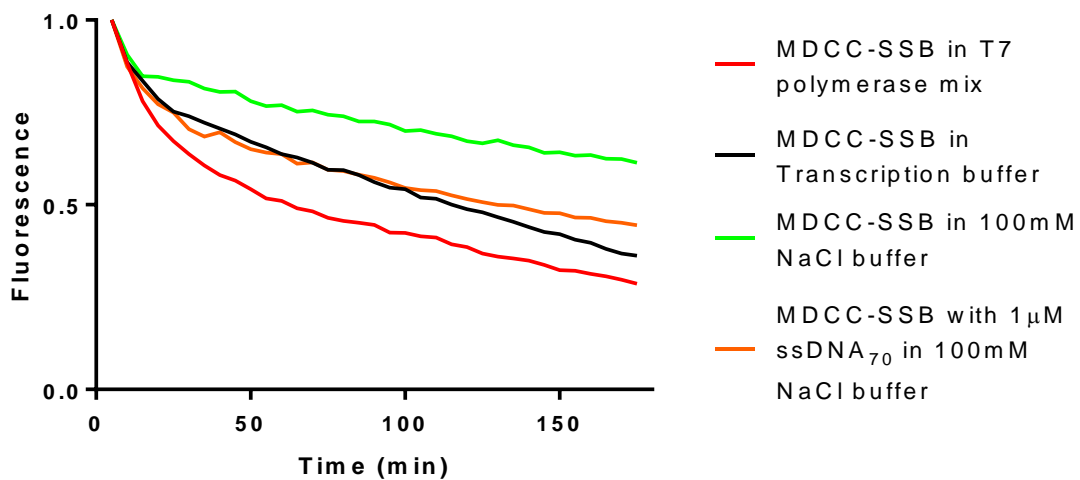


Figure 3.18. **MDCC-SSB is not a suitable biosensor for the real time analysis of transcription.** 250nM MDCC-SSB was added to the polymerase mix as stated in the TranscriptAid T7 High Yield Transcription kit, controls were also set up, 250nM MDCC-SSB alone in transcription buffer provided in the kit, 250nM alone in 100mM NaCl buffer as previously used and 250nM with 1µM ssDNA₇₀ in 100mM NaCl buffer. The transcription proceeded for 3 hours at 37°C in which a 2223nt long gene was transcribed and the MDCC-SSB emission was measured at 470nm every minute. Decrease in fluorescence occurred in all samples in a similar fashion with a rapid decrease in the first 10 minutes and a steady decrease for the remaining period of time. All samples were normalised to 1, which is the original fluorescence of MDCC-SSB in the designated buffer.

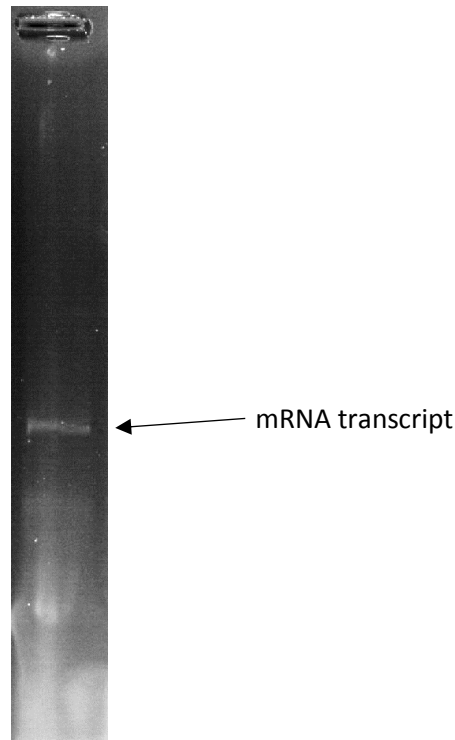


Figure 3.19. **An acrylamide gel to show the presence of mRNA from the T7 polymerase assay with MDCC-SSB.** A 100 times diluted sample taken from the MDCC-SSB transcription mix was loaded onto a 1% agarose gel in a 1X MOPS buffer and stained with SYBR Gold (no ladder was used due to the ladder provided containing Ethidium Bromide). One band was observed, suggesting the presence of mRNA transcripts.

3.7 Evaluating the loss of fluorescence

To understand the loss of fluorescence during the 3 hour transcription period at 37°C, various methods were used. Firstly, the coumarin dye MDCC does not lose any fluorescence over the 3 hours due to bleaching effects or fluorescence lifetime effects in 100mM NaCl buffer (figure 3.16).

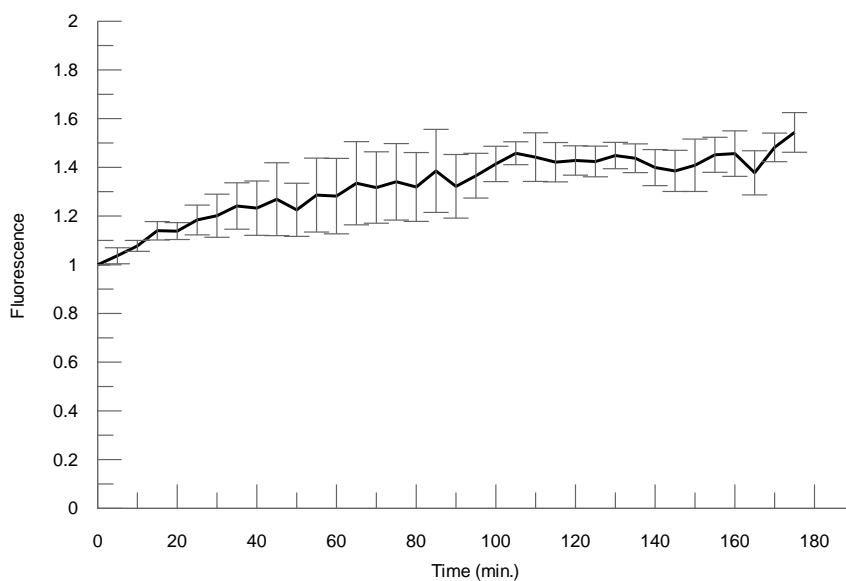


Figure 3.20. **MDCC does not lose fluorescence over 3 hours at 37°C.** 1 μ M of MDCC in 100mM NaCl buffer was incubated at 37°C for 3 hours. The emission was measured at 470nm and readings were taken every 5 minutes and plotted with standard error. Over three hours there is not a reduction in fluorescence but a gradual increase in MDCC fluorescence is observed.

Whilst there is not a decrease in fluorescence there does seem to be a slight increase over time to approximately a 1.5 fold increase. MDCC's life time or bleaching effects caused by continuous excitement can be ruled out for the loss of fluorescence.

MDCC-SSB exhibits no loss of structure over 3 hour's incubation at 37°C. To understand if the decrease in fluorescence was due to unfolding of the MDCC-SSB, as a result of labelling or instability in 100mM NaCl buffer, circular dichroism (CD) spectra were taken of SSB and MDCC-SSB (figure 3.17). After three hours of incubation there seemed to be no major change of structure of either species.

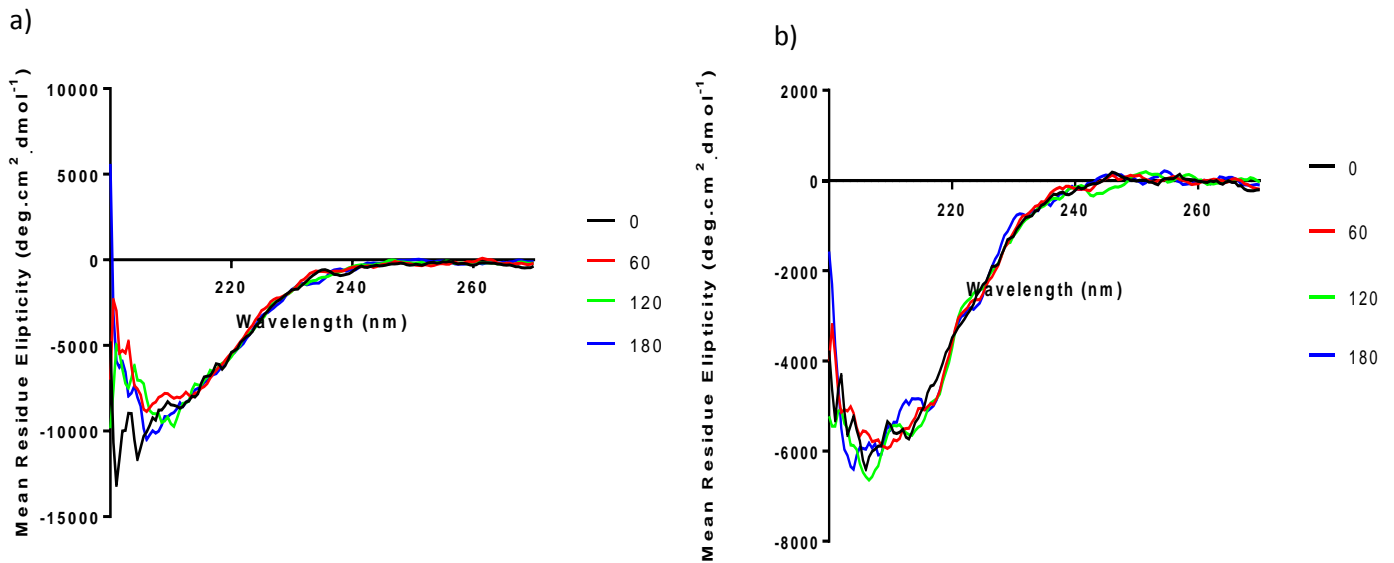


Figure 3.21. **CD spectra showing no severe loss of structure of any SSB species over 3 hours.** 0.2mg.mL⁻¹ of SSB (a), MDCC-SSB (b) were incubated for 3 hours at 37°C and measurements were taken in the far UV wavelengths (200-270) every 60 minutes.

After 3 hours of incubation CD was used to calculate the melting points of each SSB species (figure 3.18). The melting points showed no loss of stability, protein having a melting point of $69.97 \pm 0.87^\circ\text{C}$ and MDCC-SSB having a melting point of $74.44 \pm 0.92^\circ\text{C}$. The bound MDCC-SSB with ssDNA₇₀ and ssRNA₇₀ had higher melting points, suggesting that SSB/MDCC-SSB is more stable in its bound form, at $76.19 \pm 0.93^\circ\text{C}$ and $77.14 \pm 0.88^\circ\text{C}$ respectively. These high melting points support the idea that there is no loss of protein structure during the 3 hour incubation period.

Since the decrease in fluorescence is not caused by MDCC, or a loss of protein structure, dynamic light scattering analysis (DLS) was used to measure the proteins size before and after a 3 hour incubation at 37°C, to specifically look for protein aggregation (figure 3.19). The DLS data shows that the majority of the MDCC-SSB species diameter after 3 hours has increased from 14.8nm to 1.19µm, which shows that aggregation has occurred. This aggregation is the most plausible cause for the decrease in fluorescence.

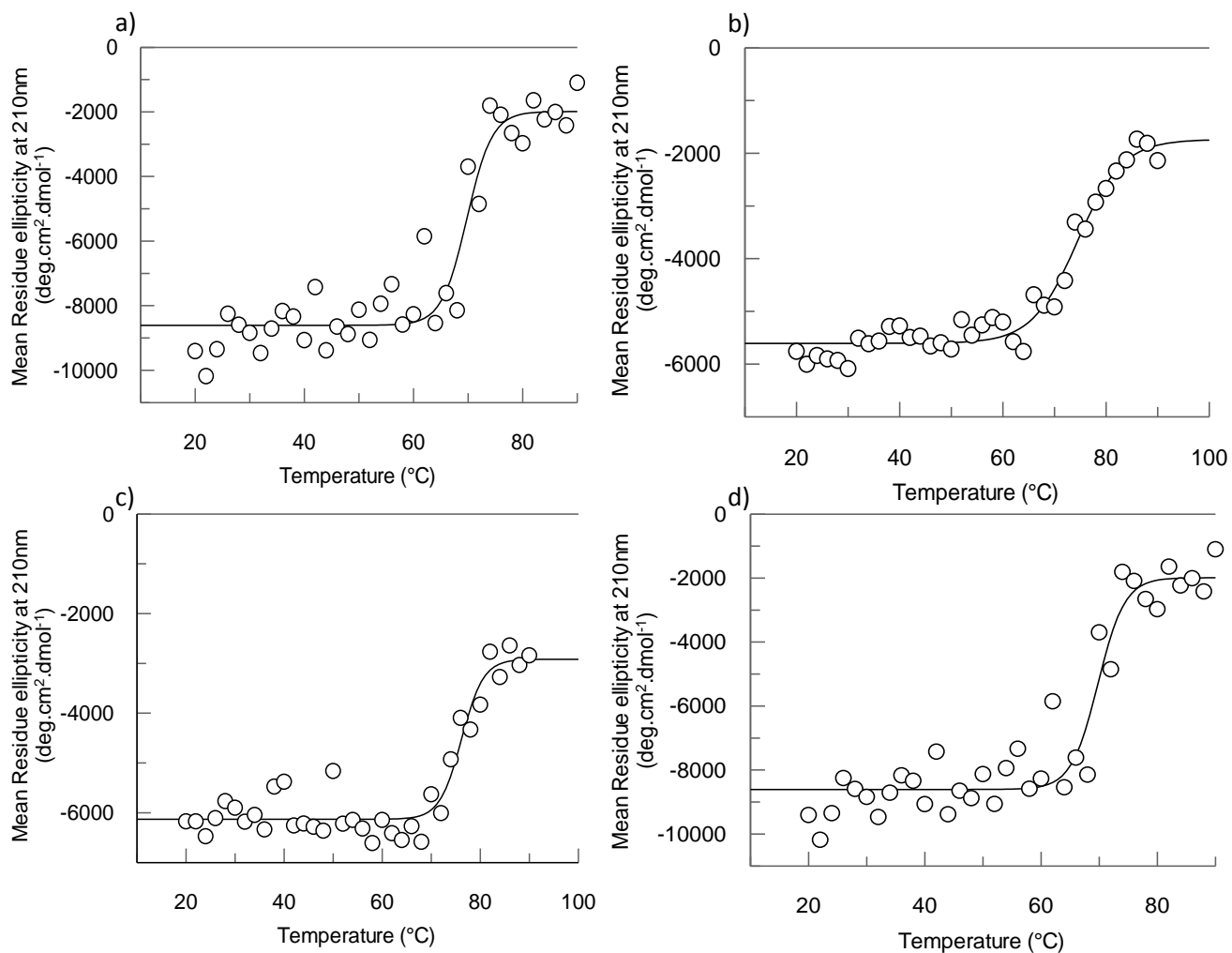


Figure 3.22. **Melting curves of SSB species.** 0.2mg.mL⁻¹ of SSB (a) and MDCC-SSB (b) after three hours of incubation were heated by 1°C for every minute. 4 readings taken at 210nm were taken for each temperature and averaged together. The same was done for MDCC-SSB bound to 0.2mg.mL⁻¹ of ssDNA₇₀ (c) and 0.2mg.mL⁻¹ of ssRNA₇₀ (d). The curves were fit with a sigmoidal Boltzmann fit, and gave the melting points, SSB=69.97±0.87°C, MDCC-SSB=74.44± 0.92°C, MDCC-SSB with ssDNA₇₀=76.19±0.93°C and MDCC-SSB with ssRNA₇₀=77.14±0.88°C.

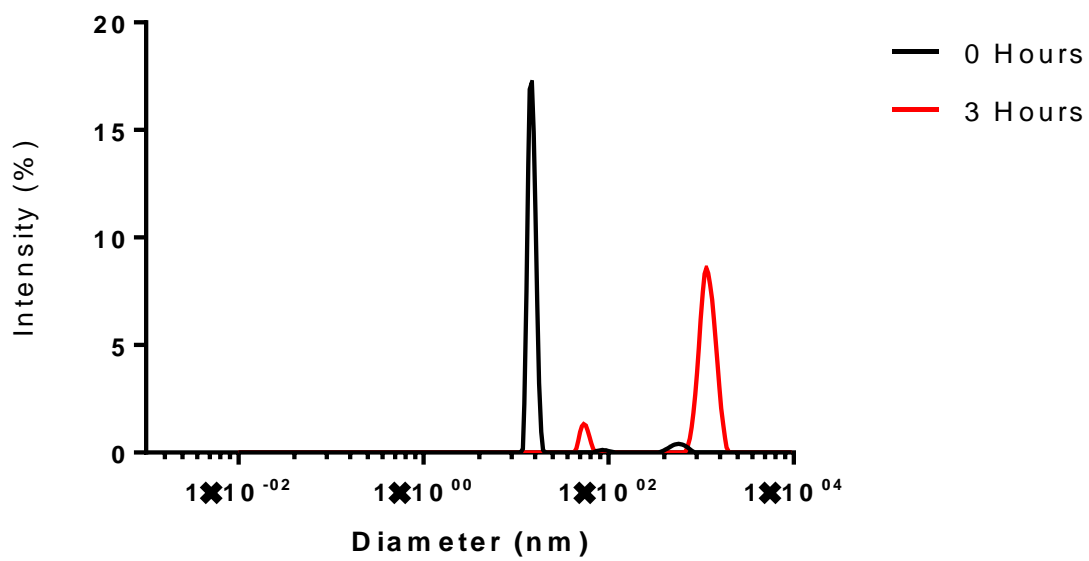


Figure 3.23. **Dynamic Light Scattering (DLS) diameter measurements of MDCC before and after a 3 hour incubation at 37°C.** 250nM of MDCC-SSB in 100mM NaCl buffer was placed in the DLS machine and diameter measurements were taken. The sample was incubated at 37°C for 3 hours and the measurement was repeated. There is a clear increase in diameters measured from 14.8nm to 1.19μm of the MDCC-SSB.

4. Discussion

Biosensors create unique opportunities to measure previously unmeasurable cell activities both *in vitro* and *in vivo*. They have provided opportunities for detecting toxins⁷⁰, quantifying glucose in cells to aid with diabetes⁷¹ and measuring enzyme kinetics⁷². This ability to manipulate biological structures and specificity is an idea that has been key to this study.

4.1 SSB can bind RNA substrates

The optimisation process of SSB purification allows the process of making this biosensor cheap and easy to reproduce. This study removed the unnecessary steps of using Polymin P precipitation and ammonium sulfate precipitation which was shown to lead to expressed protein being lost. Instead a poly-histidine tagged protein reduced the purification to a one column process resulting in the high yield of a near pure product. This process of optimisation has reduced the time needed to produce the biosensor and, therefore encourages further use in different studies.

During the production of this biosensor it was vital to compare the SSB binding to ssRNA with ssDNA. This is because SSBs role has been well characterised in binding to ssDNA⁵⁴ and so any observed results of MDCC-SSB ssDNA binding would act as a positive control throughout the production of the biosensor. This study has reinforced the idea that SSB is able to bind to multiple substrates, but favours ssDNA over ssRNA. The first studies on unlabelled SSB using EMSA, substrate titrations and thermophoresis support the idea that SSB is able to bind to both ssDNA and ssRNA. RNA binding has already been previously shown by Shimamoto *et al*⁶¹, within the context of SSB's ability to bind to its own mRNA. Whilst this has been reported it was important to reinforce this knowledge and compare the binding of both substrates that were designed to be of same lengths. As SSB binding occurs through its OB-folds, it is assumed that mRNA binding would occur, as this type of interaction does not distinguish between ssDNA and ssRNA substrates⁷³. The EMSA showed binding of both substrates and a splitting of bands due to the different SSB species binding to those substrates. However, as the

substrates were in excess not the protein, there was still some ssDNA and ssRNA that travelled freely through the gel.

The tryptophan quenching studies using the fluorescence spectrophotometer showed that binding occurs for both substrates, although tryptophan quenching was observed it was much lower than the expected 80% quenching. This could be due to the low salt concentration used compared to previous studies and the potential of background nucleotide fluorescence. Complete saturation did not occur with quenching entering a second reduced gradient linear phase. This could be because of slight conformational changes SSB undertakes over time and gentle rearrangements of the substrate within the protein and so the quoted value of percentages is not calculated knowing the 100% quenched value.

The use of thermophoresis gave a more accurate depiction of both the binding modes of SSB when binding to the two substrates. This is due to the ability of ssDNA to fluoresce within the protein-UV spectra, which can cause background fluorescence when using a simple fluorescence spectrophotometer. As thermophoresis uses a small pathlength, small quantities of SSB and is a relatively rapid procedure, there is a reduction in the error caused by internal filtering effects and bleaching effects of the tryptophan fluorescence. The observation that binding stoichiometry is different for the ssDNA and ssRNA substrates arose from the apparent K_d 's being 50nM and 134nM for ssDNA and ssRNA respectively. A 1:1 of complete SSB homotetramer to one molecule of ssDNA₇₀ stoichiometry is defined but for ssRNA a ratio of 2 SSB subunits seems to bind to 1 molecule of ssRNA₇₀. This ratio of binding implies that there are more SSB species in the (SSB)₃₅ binding mode at 150mM NaCl when with the ssRNA₇₀ compared to the (SSB)₆₅ binding mode with ssDNA₇₀ at this salt concentration. These differences in apparent K_d 's could be explained by two ssRNA₇₀ molecules binding to one SSB tetramer or that SSB is in a dimer formation when interacting with ssRNA₇₀ at this salt concentration. These binding modes need to be considered when discussing the saturation of SSB molecules with substrate as an array of SSB monomer conformations could be occurring due to the buffer or substrate composition.

Concentration dependent binding curves do not occur when using fluorescent oligonucleotides, potentially due to the short length employed in these studies. Nevertheless, this technique was utilised to show that even an “extreme” example of mRNA transcript- a transcript that contains only uracil nucleotides- can be bound by SSB. The fPolyU₂₀, a fluorescein tagged twenty uracil nucleotide RNA molecule is quenched when SSB is added to the sample. This quenching however for both the fssDNA₁₆ and the fPolyU₂₀ does not produce a distinctive binding curve when SSB is titrated into the system. The fssDNA₁₆ substrate showed a decrease in percentage of fluorescence quenched with an increase of SSB concentration, but for the fpolyU₂₀ substrate a trend is far harder to see. The explanation could be related to the length of the nucleotide strands. It is hard to predict where exactly the OB-fold will be able to bind on the nucleotides and exactly how many OB-folds will interact with these particularly short nucleotide sequences, which could lead to heterogeneous quenching of the signal within the SSB sample and explains why a binding curve is not easily observed. This is summarised in figure 4.1.

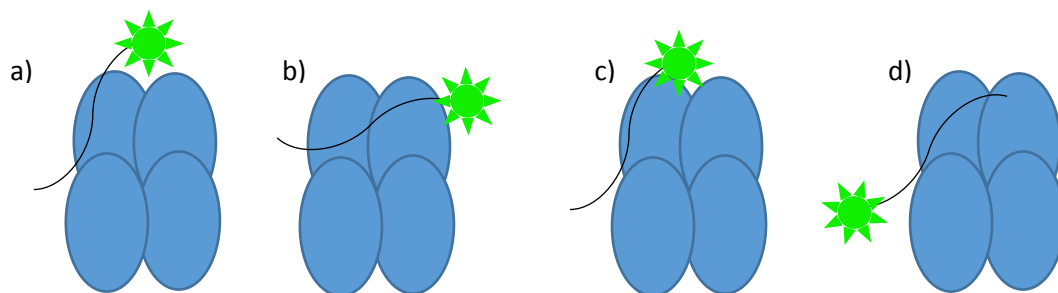


Figure 4.1. **Diagram showing potential binding conformations of short fluorescent nucleotides to SSB.** fssDNA₁₆ molecules bound to SSB with a) SSB binding the centre of the substrate. b) two monomers binding the molecule with increased quenching of the fluorescein due to proximity of protein. c) fssDNA₁₆ bound to one monomer of SSB near the fluorescein binding site causing high quenching and d) binding of the molecule to one SSB monomer at the opposite end of the fluorescein dye allowing free rotation of the fluorescein with normal fluorescence intensity.

Binding kinetics may have an effect on the biosensors reliability when measuring mRNA concentrations in a sample containing ssDNA. The competition assay showed the biosensor is not suitable to be used when a solution contains ssDNA because the fssDNA₄₀ was able to outcompete the ssRNA₇₀ for binding to the SSB. To improve this assay and to ensure all bound ssRNA can be displaced by ssDNA, it would be necessary to increase the length of the fluorescein ssDNA to match the length of the RNA used. This would prevent the SSB tetramer from binding both substrates at the same time, as SSB could be in various binding modes for substrates 40 nucleotides long. The competition assay between ssRNA₇₀ and fssDNA₄₀ reinforces the importance of a sample to not contain ssDNA.

4.2 Generating the biosensor

Labelling optimisation has led to at least three out of the four SSB monomers, each containing a single cysteine residue, to be labelled. Optimisation of labelling methods became the next priority after confirmation of mRNA binding to ensure a large enough amount of SSB subunits are labelled with MDCC to produce a viable signal. The labelling technique varied from previous protocols^{49,63} in which labelling occurred under nitrogen gas. The nitrogen in these methods act as an oxidising agent and stops the cysteine residues from forming dimers whilst labelling occurs. Although this method would ensure a higher percentage of monomer labelling, to ease the production of the MDCC-SSB biosensor it was not deemed unnecessary, as sufficient labelling occurs without it. To increase labelling efficiency of cysteine residues with MDCC, the optimisation process would need to be revisited to include nitrogen or the use of β -mercaptoethanol rather than DTT to stop disulphide bridges from forming.

The MDCC-SSB signal is stable and linear at both high and low concentrations and salt concentrations. This study shows the addition of excess ssDNA or ssRNA substrates results in a large fluorescence increase of 1.9 and 2.1 fold. This fluorescence increase is not as high as previously quoted from Dillingham *et al*⁴⁹ in which when MDCC-SSB bound ssDNA a 4.9 fold increase was observed. This variation in fluorescence could be down to reduced labelling of SSB monomers in this study in which unlabelled monomers as part of the tetramer are still able to bind but do not produce a signal. Also,

here, compared to the previous one, a lower salt concentration was used which could result in a difference in binding modes of SSB between the studies. For both substrates, the excitation maximum and emission maximum occurred at 435nm and 470nm respectively with a Stokes shift of 35nm. The fact there is no difference in these peaks implies the ssDNA and ssRNA are binding in similar way and are causing the same protein conformation changes leading to a fluorescence increase.

This result shows the biosensor is capable of reporting on the presence of ssRNA. The fluorescence increase occurs in a substrate concentration dependent manner for both the ssRNA and ssDNA substrates. Whilst it has previously been proven that this occurs with ssDNA, it was important to use the ssDNA as a positive control so as to ensure the biosensor was behaving as expected and that it was stable and responding in both high and low salt conditions. There was some difference in the saturation point of the biosensor with ssDNA₇₀, at low salt being 64nM and 90nM at high salt, showing that the biosensor is responsive in both buffers. The interesting response of the MDCC-SSB is that the saturation point occurs at a higher concentration than the expected 50nM. The higher saturation points for the ssDNA substrate could be down to the three out of four monomers labelled and the salt concentration that might be pushing the SSB into an (SSB)₃₅, in which only two OB-folds bind with the substrate. With binding modes being fluid, the MDCC-SSB solution containing the ssDNA could be a complex mix of dimers and tetramers in both binding modes. Further work would be required to define this cocktail of SSB species using, for example, Size Exclusion Chromatography with Multi-Angle Light Scattering (SEC-MALS) analysis to determine the oligomeric states. To reduce the amount of unlabelled monomers still present in the biosensor mix, a gel filtration column could be used with high separation that would allow for the isolation of the labelled species only.

This knowledge can be applied to the higher saturation points observed with ssRNA being at 101nM in low salt and 109nM in high salt. Unlike ssDNA these two saturation points seem to be independent of the salt concentration. Moreover, as with the thermophoresis, it appears that the (SSB)₃₅ binding mode may dominate for the ssRNA substrates. When ssRNA substrates are at a low concentration there is a linear increase in fluorescence before saturation of the biosensor. Saturation is the point at

which there is no free biosensor in the system. Calibration of the biosensor required 50nM MDCC-SSB in 100mM NaCl buffer. This presented a linear increase of fluorescence starting from 3.9nM of ssRNA₇₀ up to 101nM of ssRNA₇₀, during this linear phase the MDCC-SSB biosensor is “sensitive” and is able to distinguish between ssRNA concentrations. After saturation occurs, a larger concentration of MDCC-SSB is necessary to quantify higher concentrations of substrate to invoke a linear fluorescence increase. The MDCC-SSB’s response to substrate is similar to both ssDNA and ssRNA in which a linear increase is present at both high and low salt concentration. The biosensor has shown it can be calibrated in different buffers and it is suitable for mRNA quantification measurements.

4.3 Application of the biosensor

The MDCC-SSB biosensor is suitable for use as a comparative assay post transcription. Each T7 polymerase transcription proceeded for a set time period, resulting in different amounts of mRNA transcript produced. RT-qPCR allowed for accurate quantification of the mRNA transcripts and the MDCC-SSB fluorescence was measured to assess if the fluorescence increase matched the mRNA concentration. When the results of the MDCC-SSB fluorescence increase were plotted against RT-qPCR quantification, there is a clear linear correlation which shows that samples can be compared against each other and there is a clear signal that separates each amount of mRNA. There was a single result where high fluorescence increase was witnessed for a small amount of mRNA but this could be explained by the loss of mRNA during the RT-qPCR preparation process or ssDNA being present in the purified samples.

The biosensor does not appear to rely on transcripts that are of specific length. Whilst ssRNA₇₀ was used to characterise the biosensor, the post transcription result shows that multiple MDCC-SSB proteins are able to bind along the length of the transcripts. To accurately quantify the concentration of mRNA, the length of the transcript needs to be known. This knowledge is required to transfer the calibration titration of the fluorescence increase, performed with ssRNA₇₀, into a concentration of

total transcripts. With transcription in varying conditions i.e. running for different lengths of time, this approach is not possible. However, total mRNA concentration can be determined in terms of SSB binding sites which are assumed to be 70 bases. This approach is very much similar to quantification through RT-qPCR. Therefore, the MDCC-SSB can distinguish between the samples based upon absolute differences in the total number of SSB binding sites along transcripts of various lengths. This represents a low cost and significantly faster method than current mRNA quantification protocols available and it can be used without the need for mRNA purification.

MDCC-SSB is not suitable for real time analysis of *in vitro* transcription. Even with the production of mRNA there is a decrease of fluorescence over time that cannot be calibrated into the assay. This decrease is due to aggregation of MDCC-SSB as shown by the DLS analysis. Further analysis identified no loss of structure of MDCC-SSB represented by the CD data and no loss of MDCC fluorescence across a three hour incubation period. During the transcription process a greater decrease in fluorescence occurred for all controls, as well as the assay itself, when single stranded substrates were present in solution. This could be due to the MDCC-SSB polymerising with binding as well as aggregating, both of which could result in the quenching of the fluorescence signal. This represents a typical limitation of using fluorescence reporters whereby numerous factors can contribute to the overall signal.

This study shows that MDCC-SSB is a suitable biosensor for measuring mRNA concentrations after transcription and eliminates the need for incorporation of radioactively labelled nucleotides and gel electrophoresis. It can be used to compare conditions without the need for quantification or to quantify mRNA concentrations after calibration of the sensor; making it a rapid process capable of withstanding different salt buffers. This calibration of MDCC-SSB takes away the need for RT-qPCR, which has multiple steps that can all incorporate human error into the protocol. The stability of this biosensor means it is able to work without extra reagents and without RNA purification as long as the samples do not contain ssDNA. It is however not suitable to be used in any real time *in vitro* transcription assays due to its ability to aggregate over time and possible polymerisation, both of which result in a loss of fluorescence. With clear evidence that SSB is able to 1) bind mRNA, 2) produce

a detectable signal when labelled with MDCC and 3) have an increase in fluorescence dependent on mRNA concentration, this study provides a new alternative to classical methods and has successfully produced a working mRNA biosensor.

5. Further Work

- Due to the similar binding patterns observed in the EMSA, the tryptophan quenching and the identical Stokes shift it is possible that RNA binds in an identical way to ssDNA. To gain a better understanding in the way in which SSB binds to RNA, the method of point mutations within the OB-fold could identify if the RNA and ssDNA interact with SSB in a similar manner, or if the SSB structure has distinct interactions with the RNA.

- Within this piece of work it was identified that saturation of the biosensor did not occur at equal concentrations of the biosensor. This is due to the dimer, tetramer species and different binding modes of SSB. An interesting study would be to quantify the SSB species in the sample so as to get a better understanding of this delayed saturation.

- Whilst in this study 50nM SSB was titrated with single stranded substrates, to increase the MDCC-SSB's use as a biosensor it would be ideal to undertake further calibrations of the biosensor at different concentrations. This could lead to a database of fluorescence increase ratios relating to mRNA concentrations in different buffers.

- This study used samples of transcription assay that proceeded for various amounts of time. To further characterise the biosensor it would be important to use it with post transcription samples that had been undertaken in different conditions, such as with the addition of inhibitors or with different concentrations of DNA template.

- Whilst SSB was proven to bind ssRNA, it would be of interest to further identify other well characterised proteins that bind to mRNA that are suitable to be fluorescently labelled, leading to

changes in fluorescence. This could generate biosensor specific to mRNA that provides reliable results even in the presence of ssDNA.

- Due to the biosensor not being suitable for real time transcription analysis it would be important to look at other fluorescent methods for this purpose. One such method could be to measure the incorporation of fluorescently labelled nucleotides.

- MDCC is not appropriate for microscopy due to its photophysical properties, SSB labelled with Cy3b another thiol reactive dye could allow this biosensor to be used in potential single molecule studies.

6. Appendix

Table 2. RT-qPCR Primers

Name	Sequence
RecD2 forward	GGGTCAACAAAGTCCGTTTC
RecD2 reverse	GTTGACCACCCGGTACTGGTA

7. References

1. Russell, J. & Zomerdijk, J. C. B. M. The RNA polymerase I transcription machinery. *Biochem. Soc. Symp.* 203–16 (2006).
2. Carter, R. & Drouin, G. Structural differentiation of the three eukaryotic RNA polymerases. *Genomics* **94**, 388–396 (2009).
3. Vreugde, S. *et al.* Nuclear Myosin VI Enhances RNA Polymerase II-Dependent Transcription. *Mol. Cell* **23**, 749–755 (2006).
4. Arimbasseri, A. G. & Maraia, R. J. RNA Polymerase III Advances: Structural and tRNA Functional Views. (2016). doi:10.1016/j.tibs.2016.03.003
5. Sarah J. Goodfellow, J. C. B. M. Z. Basic Mechanisms in RNA Polymerase I Transcription of the Ribosomal RNA Genes. *Subcell. Biochem.* **61**, (2012).
6. Marilyn N. Szentirmay, M. S. Spatial organization of RNA polymerase II transcription in the nucleus. *Nucleic Acids Res.* **28**, 2019 (2000).
7. Pombo, A. *et al.* Regional specialization in human nuclei: visualization of discrete sites of transcription by RNA polymerase III. *EMBO J.* **18**, 2241–53 (1999).
8. Brégeon, D. & Doetsch, P. W. Transcriptional mutagenesis: causes and involvement in tumour development. *Nat. Rev. Cancer* **11**, 218–27 (2011).
9. Tao, H. *et al.* Emerging role of long noncoding RNAs in lung cancer: Current status and future prospects. *Respir. Med.* **110**, 12–19 (2016).
10. Hofmann, W. A., Johnson, T., Klapczynski, M., Fan, J.-L. & de Lanerolle, P. From transcription to transport: emerging roles for nuclear myosin I. *Biochem. Cell Biol.* **84**, 418–26 (2006).
11. Sainsbury, S., Bernecky, C. & Cramer, P. Structural basis of transcription initiation by RNA polymerase II. *Nat. Rev. Mol. Cell Biol.* **16**, 129–143 (2015).
12. Plaschka, C. *et al.* Transcription initiation complex structures elucidate DNA opening. *Nature* **533**, 353–358 (2016).
13. Mandal, S. S. *et al.* Functional interactions of RNA-capping enzyme with factors that positively and negatively regulate promoter escape by RNA polymerase II. *Proc. Natl. Acad. Sci.* **101**, 7572–7577 (2004).
14. Goodrich, J. A. & Tjian, R. Transcription factors IIE and IIH and ATP hydrolysis direct promoter clearance by RNA polymerase II. *Cell* **77**, 145–156 (1994).
15. Revyakin, A., Liu, C., Ebright, R. H. & Strick, T. R. Abortive initiation and productive initiation by RNA polymerase involve DNA scrunching. *Science* **314**, 1139–43 (2006).
16. Bywater, M. J., Pearson, R. B., McArthur, G. A. & Hannan, R. D. Dysregulation of the basal RNA polymerase transcription apparatus in cancer. *Nat. Rev. Cancer* **13**, 299–314 (2013).
17. Schweikhard, V. *et al.* Transcription factors TFIIIF and TFIIIS promote transcript elongation by RNA polymerase II by synergistic and independent mechanisms. *Proc. Natl. Acad. Sci. U. S. A.* **111**, 6642–7 (2014).
18. Bushnell, D. A., Cramer, P. & Kornberg, R. D. Structural basis of transcription: α -Amanitin-RNA polymerase II cocrystal at 2.8 Å resolution. *Proc. Natl. Acad. Sci.* **99**, 1218–1222 (2002).
19. Milligan, J. F. & Uhlenbeck, O. C. Synthesis of small RNAs using T7 RNA polymerase. *Methods in Enzymology* **180**, 51–62 (1989).

20. Jani, B. & Fuchs, R. In vitro transcription and capping of Gaussia luciferase mRNA followed by HeLa cell transfection. *J. Vis. Exp.* (2012). doi:10.3791/3702
21. Warren, L. *et al.* Highly efficient reprogramming to pluripotency and directed differentiation of human cells with synthetic modified mRNA. *Cell Stem Cell* **7**, 618–30 (2010).
22. Cwakraborty, P. R., Bandyopadhyay, P., Huang, H. H. & Maitra, U. Fidelity of in Vitro Transcription of T3 Deoxyribonucleic Acid by Bacteriophage T3-induced Ribonucleic Acid Polymerase and by Escherichia coli Ribonucleic Acid Polymerase*. *J. Biol. Chem.* **249**, 6901–6909 (1974).
23. Köhrer, C., Mayer, C., Gröbner, P. & Piendl, W. Use of T7 RNA polymerase in an optimized Escherichia coli coupled in vitro transcription-translation system. Application in regulatory studies and expression of long transcription units. *Eur. J. Biochem.* **236**, 234–9 (1996).
24. Stump, W. T. & Hall, K. B. SP6 RNA polymerase efficiently synthesizes RNA from short double-stranded DNA templates. *Nucleic Acids Res.* **21**, 5480–4 (1993).
25. Dignam, J. D., Lebovitz, R. M. & Roeder, R. G. Accurate transcription initiation by RNA polymerase II in a soluble extract from isolated mammalian nuclei. *Nucleic Acids Res.* **11**, 1475–89 (1983).
26. Desjardins, P. & Conklin, D. NanoDrop microvolume quantitation of nucleic acids. *J. Vis. Exp.* (2010). doi:10.3791/2565
27. Huang, C. & Yu, Y.-T. Synthesis and labeling of RNA in vitro. *Curr. Protoc. Mol. Biol.* **Chapter 4**, Unit4.15 (2013).
28. Heid, C. A., Stevens, J., Livak, K. J. & Williams, P. M. Real time quantitative PCR. *Genome Res.* **6**, 986–94 (1996).
29. Voss, C. *et al.* A novel, non-radioactive eukaryotic in vitro transcription assay for sensitive quantification of RNA polymerase II activity. *BMC Mol. Biol.* **15**, 7 (2014).
30. Jones, L. J., Yue, S. T., Cheung, C.-Y. & Singer, V. L. RNA Quantitation by Fluorescence-Based Solution Assay: RiboGreen Reagent Characterization. *Anal. Biochem.* **265**, 368–374 (1998).
31. Ilgu, M. *et al.* Light-up and FRET aptamer reporters; evaluating their applications for imaging transcription in eukaryotic cells. *Methods* (2015). doi:10.1016/j.ymeth.2015.12.009
32. Sando, S., Narita, A., Hayami, M. & Aoyama, Y. Transcription monitoring using fused RNA with a dye-binding light-up aptamer as a tag: a blue fluorescent RNA. *Chem Commun* 3858–3860 (2008). doi:10.1039/b808449a
33. Murphy, D. Nuclear run-on analysis of transcription. *Methods Mol. Biol.* **18**, 355–61 (1993).
34. Marras, S. A. E., Gold, B., Kramer, F. R., Smith, I. & Tyagi, S. Real-time measurement of in vitro transcription. *Nucleic Acids Res.* **32**, e72 (2004).
35. Niederholtmeyer, H., Xu, L. & Maerkl, S. J. Real-Time mRNA Measurement during an in Vitro Transcription and Translation Reaction Using Binary Probes. *ACS Synth. Biol.* 121221093752004 (2012). doi:10.1021/sb300104f
36. Kocaoglu, O. & Carlson, E. E. Progress and prospects for small-molecule probes of bacterial imaging. *Nat. Chem. Biol.* **12**, 472–8 (2016).
37. Patel, J. T., Belsham, H. R., Rathbone, A. J. & Friel, C. T. Use of stopped-flow fluorescence and labeled nucleotides to analyze the ATP turnover cycle of kinesins. *J. Vis. Exp.* e52142 (2014). doi:10.3791/52142

38. Salins, L. L. E., Deo, S. K. & Daunert, S. Phosphate binding protein as the biorecognition element in a biosensor for phosphate. *Sensors Actuators, B Chem.* **97**, 81–89 (2004).
39. Biro, F. N., Zhai, J., Doucette, C. W. & Hingorani, M. M. Application of stopped-flow kinetics methods to investigate the mechanism of action of a DNA repair protein. *J. Vis. Exp.* (2010). doi:10.3791/1874
40. Zhao, H., Mayer, M. L. & Schuck, P. Analysis of protein interactions with picomolar binding affinity by fluorescence-detected sedimentation velocity. *Anal. Chem.* **86**, 3181–7 (2014).
41. Eric A. Nalefski, *, Eugene Nebelitsky, Janice A. Lloyd, and & Gullans‡, S. R. Single-Molecule Detection of Transcription Factor Binding to DNA in Real Time: Specificity, Equilibrium, and Kinetic Parameters. (2006).
42. Fili, N. & Toseland, C. P. in 1–24 (Springer Basel, 2014). doi:10.1007/978-3-0348-0856-9_1
43. Nagel, B., Dellweg, H. & Gierasch, L. M. Glossary for chemists of terms used in biotechnology (IUPAC Recommendations 1992). *Pure Appl. Chem.* **64**, 143–168 (1992).
44. Salins, L. L. E., Goldsmith, E. S., Ensor, C. M. & Daunert, S. A fluorescence-based sensing system for the environmental monitoring of nickel using the nickel binding protein from *Escherichia coli*. *Anal. Bioanal. Chem.* **372**, 174–180 (2002).
45. Ruscito, A. & DeRosa, M. C. Small-Molecule Binding Aptamers: Selection Strategies, Characterization, and Applications. *Front. Chem.* **4**, 14 (2016).
46. Menti, C., Henriques, J. A. P., Missell, F. P. & Roesch-Ely, M. Antibody-based magneto-elastic biosensors: potential devices for detection of pathogens and associated toxins. *Appl. Microbiol. Biotechnol.* (2016). doi:10.1007/s00253-016-7624-3
47. Brune, M. *et al.* Mechanism of inorganic phosphate interaction with phosphate binding protein from *Escherichia coli*. *Biochemistry* **37**, 10370–80 (1998).
48. Brune, M., Hunter, J. L., Corrie, J. E. & Webb, M. R. Direct, real-time measurement of rapid inorganic phosphate release using a novel fluorescent probe and its application to actomyosin subfragment 1 ATPase. *Biochemistry* **33**, 8262–71 (1994).
49. Dillingham, M. S. *et al.* Fluorescent single-stranded DNA binding protein as a probe for sensitive, real-time assays of helicase activity. *Biophys. J.* **95**, 3330–9 (2008).
50. Fili, N. *et al.* Visualizing helicases unwinding DNA at the single molecule level. *Nucleic Acids Res.* **38**, 4448–4457 (2010).
51. Morten, M. J. *et al.* Binding dynamics of a monomeric SSB protein to DNA: a single-molecule multi-process approach. *Nucleic Acids Res.* 1–18 (2015). doi:10.1093/nar/gkv1225
52. Flynn, R. L. & Zou, L. Oligonucleotide/oligosaccharide-binding fold proteins: a growing family of genome guardians. *Crit. Rev. Biochem. Mol. Biol.* **45**, 266–75 (2010).
53. Antony, E. *et al.* Multiple C-terminal tails within a single *E. coli* SSB homotetramer coordinate DNA replication and repair. *J. Mol. Biol.* **425**, 4802–19 (2013).
54. Lohman, T. M. & Ferrari, M. E. *Escherichia Coli* Single-Stranded DNA-Binding Protein: Multiple DNA-Binding Modes and Cooperativities. *Annu. Rev. Biochem.* **63**, 527–570 (1994).
55. Bujalowski, W., Overman, L. B. & Lohman, T. M. Binding mode transitions of *Escherichia coli* single strand binding protein-single-stranded DNA complexes. Cation, anion, pH, and binding density effects. *J. Biol. Chem.* **263**, 4629–40 (1988).

56. Kozlov, A. G. & Lohman, T. M. E. coli SSB tetramer binds the first and second molecules of (dT)₃₅ with heat capacities of opposite sign. *Biophys. Chem.* **159**, 48–57 (2011).
57. Waldman, V. M., Weiland, E., Kozlov, A. G. & Lohman, T. M. Is a fully wrapped SSB-DNA complex essential for Escherichia coli survival? *Nucleic Acids Res.* **44**, 4317–29 (2016).
58. Raghunathan, S., Kozlov, A. G., Lohman, T. M. & Waksman, G. Structure of the DNA binding domain of E. coli SSB bound to ssDNA. *Nat. Struct. Biol.* **7**, 648–652 (2000).
59. Ferrari, M. E., Bujalowski, W. & Lohman, T. M. Co-operative binding of Escherichia coli SSB tetramers to single-stranded DNA in the (SSB)₃₅ binding mode. *J. Mol. Biol.* **236**, 106–123 (1994).
60. Kunzelmann, S., Morris, C., Chavda, A. P., Eccleston, J. F. & Webb, M. R. Mechanism of interaction between single-stranded DNA binding protein and DNA. *Biochemistry* **49**, 843–852 (2010).
61. Shimamoto, N., Ikushima, N., Utiyama, H., Tachibana, H. & Horie, K. Specific and cooperative binding of E. coli single-stranded DNA binding protein to mRNA. *Nucleic Acids Res.* **15**, 5241–50 (1987).
62. Froger, A. & Hall, J. E. Transformation of plasmid DNA into E. coli using the heat shock method. *J. Vis. Exp.* 253 (2007). doi:10.3791/253
63. Green, M. *et al.* Engineering a reagentless biosensor for single-stranded DNA to measure real-time helicase activity in Bacillus. *Biosens. Bioelectron.* **61**, 579–586 (2014).
64. Casas-Finet, J. R., Khamis, M. I., Maki, A. H. & Chase, J. W. Tryptophan 54 and phenylalanine 60 are involved synergistically in the binding of E. coli SSB protein to single-stranded polynucleotides. *FEBS Lett.* **220**, 347–352 (1987).
65. Lohman, T. M., Overman, L. B., Ferrari, M. E. & Kozlov, a. G. A highly salt-dependent enthalpy change for Escherichia coli SSB protein- nucleic acid binding due to ion-protein interactions. *Biochemistry* **35**, 5272–5279 (1996).
66. Molineux, I. J., Pauli, A. & Gefter, M. L. Physical studies of the interaction between the Escherichia coli DNA binding protein and nucleic acids. *Nucleic Acids Res.* **2**, 1821–37 (1975).
67. Jerabek-Willemsen, M., Wienken, C. J., Braun, D., Baaske, P. & Duhr, S. Molecular interaction studies using microscale thermophoresis. *Assay Drug Dev. Technol.* **9**, 342–53 (2011).
68. Slatter, A. F., Thomas, C. D. & Webb, M. R. PcrA helicase tightly couples ATP hydrolysis to unwinding double-stranded DNA, modulated by the initiator protein for plasmid replication, RepD. *Biochemistry* **48**, 6326–34 (2009).
69. Jerabek-Willemsen, M. *et al.* MicroScale Thermophoresis: Interaction analysis and beyond. *J. Mol. Struct.* **1077**, 101–113 (2014).
70. McPartlin, D. A., Lochhead, M. J., Connell, L. B., Doucette, G. J. & O’Kennedy, R. J. Use of biosensors for the detection of marine toxins. *Essays Biochem.* **60**, 49–58 (2016).
71. Klueh, U. *et al.* Basement Membrane-Based Glucose Sensor Coatings Enhance Continuous Glucose Monitoring in Vivo. *J. Diabetes Sci. Technol.* **9**, 957–65 (2015).
72. Huang, Y., Zhang, Q., Liu, G. & Zhao, R. A continuous-flow mass biosensor for the real-time dynamic analysis of protease inhibition. *Chem. Commun. (Camb).* **51**, 6601–4 (2015).
73. Angelica, M. D. & Fong, Y. Nucleic Acid Recognition by OB-Fold Proteins. *October* **141**, 520–529 (2008).

